

A Study in Model Based Control of an Evaporative Emissions Management System

Examensarbete utfört i Fordonssystem
vid Tekniska Högskolan i Linköping
av

Jonas Jerrelind

Reg nr: LiTH-ISY-EX-1893

A Study in Model Based Control of an Evaporative Emissions Management System

Examensarbete utfört i Fordonssystem
vid Tekniska Högskolan i Linköping
av

Jonas Jerrelind

Reg nr: LiTH-ISY-EX-1893

Supervisor: **Mattias Nyberg**

Examiner: **Lars Nielsen**

Linköping, 9th April 1998.



Avdelning, Institution
Division, department
Department of Electrical Engineering
Division of Vehicular Systems

Datum
Date
1998-04-09

Språk
Language

Svenska/Swedish
 Engelska/English

Rapporttyp
Report: category

Licentiatavhandling
 Examensarbete
 C-uppsats
 D-uppsats
 Övrig rapport

ISBN

ISRN

Serietitel och serienummer **ISSN**
Title of series, numbering

LiTH-ISY-EX- 1893

URL för elektronisk version

Titel En studie i modellbaserad reglering av ett system för begränsning av utsläpp av förångat bränsle
Title

A Study in Model Based Control of an Evaporative Emissions Management System

Författare Jonas Jerrelind
Author

Sammanfattning
Abstract

Current environmental problems such as formation of smog and ozone in cities mainly originate from emissions of hydrocarbons released by the transportation sector. Therefore authorities have, mainly in the USA and the EU, mandated both lower exhaust emissions standards and more stringent evaporative emissions test procedures for vehicles.

In order to reduce the evaporative emissions from the fuel tank, most modern cars use an evaporative emissions management system. However, without careful control of the system, exhaust emissions can increase.

Here a control method is presented for an evaporative emissions management system. The control method is based on a model of a spark-ignited (SI) engine and a model of an evaporative emissions management system. Included in the control method are estimations of the vapour flow and composition of air and fuel in the vapour from the evaporative emissions management system. The estimates are thereafter used in an improved fuel control algorithm in order to reduce the exhaust emissions.

The improved fuel control algorithm is simulated and validated together with a model of an SI-engine. Simulations show that the control method presented might substantially improve the exhaust emissions control.

A closer study of the carbon canister, a part of the evaporative emissions management system, is also presented.

Nyckelord
Keywords

evaporative emissions, carbon canister, model based control, adsorption, exhaust emissions, SI-engine, purge control valve, physical modelling

Abstract

Current environmental problems such as formation of smog and ozone in cities mainly originate from emissions of hydrocarbons released by the transportation sector. Therefore authorities have, mainly in the USA and the EU, mandated both lower exhaust emissions standards and more stringent evaporative emissions test procedures for vehicles.

In order to reduce the evaporative emissions from the fuel tank, most modern cars use an *evaporative emissions management system*. However, without careful control of the system, exhaust emissions can increase.

Here a control method is presented for an evaporative emissions management system. The control method is based on a model of a spark-ignited (SI) engine and a model of an evaporative emissions management system. Included in the control method are estimations of the vapour flow and composition of air and fuel in the vapour from the evaporative emissions management system. The estimates are thereafter used in an improved fuel control algorithm in order to reduce the exhaust emissions.

The improved fuel control algorithm is simulated and validated together with a model of an SI-engine. Simulations show that the control method presented might substantially improve the exhaust emissions control.

A closer study of the carbon canister, a part of the evaporative emissions management system, is also presented.

Keywords: evaporative emissions, carbon canister, model based control, adsorption, exhaust emissions, SI-engine, purge control valve, physical modeling

Acknowledgments

This work have been carried out at the division of Vehicular Systems, Linköping University. I would like to thank all at Vehicular Systems for a stimulating and pleasant time. I would especially like to thank my supervisor Mattias Nyberg for giving me many good ideas and all the support I needed during this work, and Andrej Perkovic for helping me with the experimental setup and the running of the experiments. Erik Frisk also deserves a credit for his help with L^AT_EX. Finally I would like to thank my family and friends for moral support during this work.

Linköping, 9th April 1998.

Jonas Jerrelind

Notation

Symbols

A	Area [m ²]
(A/F)	Air/fuel ratio
$(A/F)_s$	Stoichiometric air/fuel ratio
c	Concentration of fuel in carbon canister [mole/m ³]
c_v	Specific heat under constant volume [J/kgK]
c_p	Specific heat under constant pressure [J/kgK]
C	Constant of intake manifold dynamics [J/m ³ mole]
C_d	Discharge coefficient
d_λ	Output of λ -controller
D	Dispersion constant [s/m ²]
J	Moment of inertia [kgm ²]
m	Mass [g]
M	Torque [Nm]
M_{air}	Molecule weight of air [g/mole]
M_{fuel}	Molecule weight of fuel [g/mole]
n	Mole number [mole]
N	Engine speed [rpm]
p	Pressure [kPa]
P	Power [W]
Q_{HV}	Heating value of gasoline [MJ/kg]
R	Specific gas constant [J/kgK]
\tilde{R}	Universal gas constant [J/kmolK]
t	Time [s]
t_c	Time delay of ignition in cylinders [s]
t_d	Time delay in λ -sensor [s]
T	Temperature [K]
u	PWM control signal [ms]
v	Velocity [m/s]
X	Constant used in the fuel dynamics
α	Throttle angle [°]
κ	Ratio of specific heats
λ	Normalized air/fuel ratio
μ	Mass concentration in fuel vapor
η_f	Fuel conversion efficiency
τ_f	Time constant in the fuel dynamics [s]
τ_λ	Time constant in the λ -sensor dynamics [s]
ω	Angular velocity [rad/s]
χ	Concentration of adsorbed fuel in the carbon canister [mole/m ³]

Frequently used subscripts

<i>a</i>	Air
<i>c</i>	Cylinder
<i>est</i> or $\hat{}$	Estimate
<i>f</i>	Fuel
<i>i</i>	Injection
<i>man</i>	Intake manifold
<i>p</i>	Purge control valve
<i>r</i>	Intake runner
<i>th</i>	Throttle

Contents

1	Introduction	1
1.1	Objective and Outline	2
2	Experimental Setup	5
2.1	EVAP System	5
2.2	Data Collection	7
3	Model of the SI-engine including the EVAP System	11
3.1	The SI-engine	11
3.1.1	The Air/Fuel Ratio	13
3.1.2	The Structure of the Model	14
3.2	Gas Dynamics	15
3.2.1	Air Flow past Throttle	16
3.2.2	Gas Flow through Purge Control Valve	16
3.2.3	Gas Flow through Intake Runners	19
3.3	Fuel Dynamics	20
3.4	Crankshaft Dynamics	20
3.5	λ -sensor Dynamics	21
4	Gas Flow Estimation Method	23
4.1	Estimation of Gas Flow from the EVAP System	24
4.2	Derivation of Steady State Relations	25
4.3	Estimation of Concentration in the Vapour Flow	26
5	Fuel Control Algorithm	29
6	Carbon Canister	31
6.1	Adsorption and Activated Carbon	31
6.1.1	Physical Adsorption	32
6.1.2	Isotherms	32
6.1.3	Dynamic Adsorption and Concentration Profiles	34
6.2	Analytical Approach to Model the Canister	35
6.3	Measurement on the Carbon Canister	37
6.3.1	Preparation and Setup of Measurement	38
6.3.2	Experimental Results	39
7	Simulations	43
7.1	Simple Fuel Control	44
7.2	Improved Fuel Control	45
8	Conclusions	51
8.1	Further Work and Extensions	52

Chapter 1

Introduction

Considering all major *anthropogenic*¹ source categories combined, except agriculture, the transportation sector releases about one third of the total emissions of hydrocarbons (HC) [9]. It has been known for some time now that HC play a major role in the formation of smog and ozone. Smog and ozone are environmental problems of great concern because they have severe health effects on humans and also because of their effects on plants and animals.

Most of the HC emissions from a modern car are from the tailpipe, but a considerable part also comes from evaporative losses in the fuel tank. From [4] it can be found that 10-30 % of the total emissions of volatile organic compounds (VOC)² from cars comes from evaporative losses. In 1970, California was the first to impose quantity limits on evaporative emissions that were followed by federal administration Degobert [4]. Current US government regulations have mandated both lower exhaust emissions standards and more stringent evaporative emissions test procedures [6]. The EU tends to follow the same limits. The limits universally adopted are 2 g HC/test. Test methods used are the Sealed Housing for Evaporative Determination (SHED) method and a trap technique method using one or several *activated carbon canisters*. In both cases, the emissions are measured during a laboratory test sequence simulating the running of the vehicle on an urban circuit during summer months [4]. In 1998, 100 % of California vehicles and 90 % of all US vehicles have to comply with new enhanced evaporative emissions procedures. For the low (LEV) and ultra low emission vehicles (ULEV), soon to be introduced in California [6], the procedures and emissions standards will be even further enhanced.

In older cars, fuel vapours in the tank is released directly to the atmosphere through a vent in the fuel-tank filler-cap. Most modern cars use an *evaporative emissions management* (EVAP) system to reduce these emissions. The basic function of an EVAP system is to trap and store the fuel vapours from the fuel tank in a canister until the engine is started. Thereafter the trapped fuel

¹Man made, caused by the human race

²Approximately the same as HC here

vapours is drawn into the engine by intake vacuum and combusts. To control the flow of vapours into the engine, a purge control valve is used, see Figure 2.3 in Chapter 2 for further details.

The canister is filled with activated carbon where the vapours can adsorb. The use of activated carbon as an adsorbent has a long history. Scheele 1742-1786, the famous Swedish chemist, made the first described experiments on gases exposed to carbon in 1773 [3]. Activated carbon is by far the most used adsorbent for emission control of organic solvents, odors, toxic gases and fuel vapours.

Since almost all modern cars are equipped with an exhaust emissions control system including a catalytic converter, EGR valve, EVAP system etc., it may look like HC emissions from the car is nearly eliminated. In practice that is not true. There are at least two factors that cause the management systems to fail. The factors are:

- Even if the carbon in the canister can adsorb a big amount of fuel vapours it still gets saturated after a while. After the canister is saturated, it releases fuel vapours to the atmosphere as if there were an open pipe straight from the fuel tank. The ways to meet this problem is to make the canister big enough so the canister will not be full under normal use of the car and also to be able to purge aggressively, i.e. to purge larger quantities of fuel vapour so that the canister will be emptied each time the car is used.
- The catalytic converter requires a air/fuel mixture close to *stoichiometric*³ for optimal working capacity. The mixture and mass flow from the canister are unknown and therefore makes the air/fuel mixture to deviate from the stoichiometric value. Under steady state conditions this can be controlled by a closed loop λ -control⁴ to keep the mixture close to stoichiometric, but under acceleration and retardation or when the purge control valve is opened and closed, the closed loop λ -control is too slow to compensate for the fast changes in mass flow. It's also difficult to purge aggressively because of the large quantities of fuel vapour which the closed loop λ -control have to compensate for.

1.1 Objective and Outline

With an objective to improve the λ -control, i.e. the exhaust emissions control, on cars equipped with an EVAP system, it would be desirable to have an estimate of mass flow and mixture of the fuel vapours from the canister so that a direct compensation could be done (without involving the λ -control). Since a direct compensation is made the ability to purge more aggressively is improved also.

³Just enough oxygen to burn all the fuel

⁴ λ , and the concepts of λ -control will be discussed in Chapter 3 and Chapter 5

The goal with this thesis is to develop a method to estimate the mass flow and mixture of the vapours from the carbon canister in order to improve the λ -control

The experiments are performed on a turbo-charged SAAB production engine equipped with an EVAP system. In Chapter 2, the experimental setup is described along with the measurement system.

In Chapter 3, a model of the engine is developed and described, including parts of the EVAP system. The carbon canister is here excluded. A method estimating the mass flow and mixture of the vapours from the carbon canister, based on the model in Chapter 3, is developed in Chapter 4. The method is then used in an improved fuel control algorithm, described in Chapter 5. The method is also used in the measurements described in Chapter 3 and 6.

The physics behind the carbon canister and an approach to model it is discussed in Chapter 6. This is made to get a broader understanding of the EVAP system. The intention was from the beginning to be able to simulate this model together with the model in Chapter 3, but the work came to a point where a delimitation was needed. In order to go further with other parts of the thesis, it was decided not to go any further with the carbon canister model.

Validation of the improved fuel control algorithm is done by simulations in Chapter 7. Finally, in Chapter 8 the conclusions are made and extensions and further work are discussed.

Chapter 2

Experimental Setup

All experiments were performed on a 4 cylinders, 2.3 liters turbo-charged spark-ignited (SI) SAAB production engine equipped with the US version of an EVAP system. The engine and the EVAP system are constructed for the SAAB 9-5 model. The engine is mounted in a test bench together with a DYNAS NT 85 AC dynamometer from Schenk. The fuel tank with the EVAP system is shown in Figure 2.1 and the engine is shown in Figure 2.2.

2.1 EVAP System

The EVAP system is illustrated in Figure 2.3. The EVAP system consists of a carbon canister, a diagnosis valve, a purge control valve and additional hoses to the system. The EVAP system is mounted together with the fuel tank.

When fuel evaporates in the fuel tank, it is led through a hose to the carbon canister. The activated carbon in the canister adsorbs the fuel vapours and clean air passes by the open diagnosis valve. When the engine is started and the purge control valve is opened, fresh air will be drawn through the diagnosis valve, used as an air vent, and the canister via the purge control valve and a back-pressure valve into the intake manifold of the engine. Along with fresh air, fuel vapours will be drawn into the engine and combust.

The carbon canister is developed by Delphi Energy & Engine Management Systems in Rochester, New York for General Motors, and is used by the different car companies within General Motors on the US market. The carbon canister is shown in Figure 2.4. A little bit simplified it consists of a canister body of black toughened nylon, with an inner retainer-screen of steel filled with wood based activated carbon, also called activated charcoal, of a nominal bed volume of 1850 cm³. The canister has three connections, a tank tube connector where the fuel vapours enter the canister, an air vent tube connector and a purge tube connector from which the vapours will be drawn into the engine. Also see Figure 2.3.



Figure 2.1: The fuel tank with the EVAP system mounted to it. The carbon canister is seen at the left of fuel tank and the diagnosis valve is the white thing next to the fuel filling-pipe.

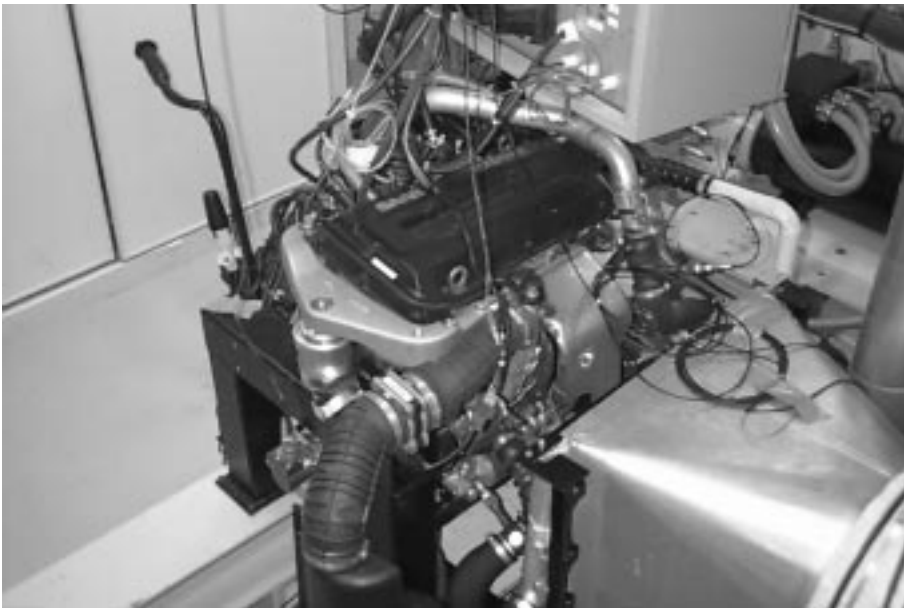


Figure 2.2: A picture of the SAAB 9-5 turbo-charged engine from above.

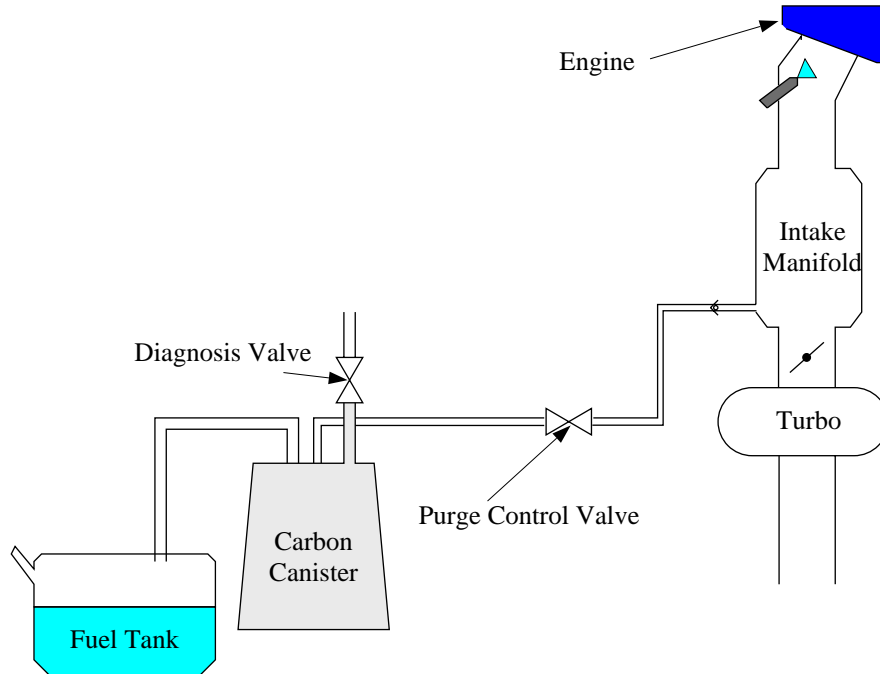


Figure 2.3: Schematic illustration of the EVAP system.

The purge control valve is a solenoid valve of type Freudenberg CPV 30C 4.0. The purge control valve is shown in Figure 2.5. A PWM¹-signal of 12 V and 8 Hz controls the open valve area. The valve is closed when no voltage is applied to it [17].

In the experiments described in this thesis the back-pressure valve is removed to simplify the experiments. The dynamometer limits the output torque to 100 Nm. This limitation will make the turbo-charger to have so little effect on the engine so it can be neglected during the experiments and the intake manifold pressure can therefore never exceed the ambient pressure. The fuel tank was only used to load the carbon canister with fuel vapours and is not connected to the engine. Fuel for the fuel injection in the engine is separately taken from a fuel tank especially designed for the engine test cell.

2.2 Data Collection

In Figure 2.6 the configuration of the control and measurement system used in the experiments is illustrated. Data were taken from the SAAB engine

¹Pulse Width Modulated



Figure 2.4: The carbon canister.



Figure 2.5: A picture of the purge control valve.

management system, Trionic T7 and its standard sensors, and from additional sensors. A CAN²-bus was used for communication with Trionic T7. The analog signals from the additional sensors were collected by an A/D-card mounted in a standard PC. All analog signals were filtered with a LP-filter with a cutoff frequency less than half the sample rate.

²Controller Area Network

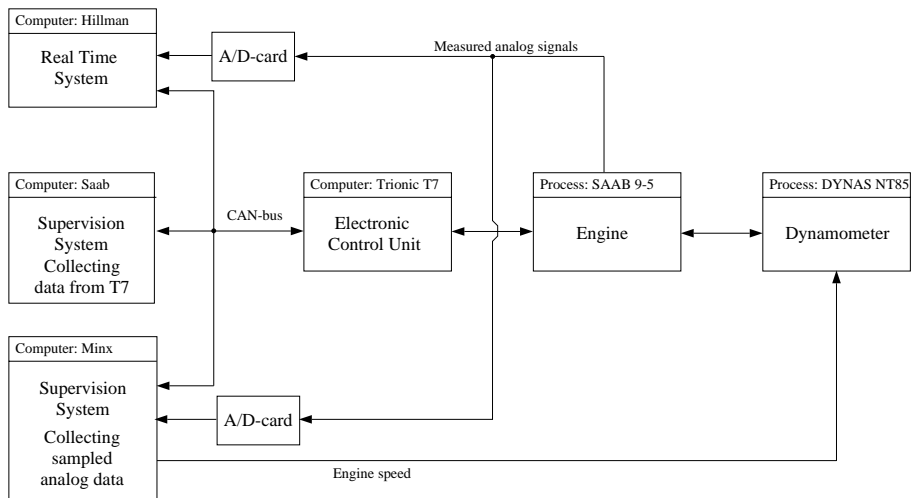


Figure 2.6: Configuration of control and measurement system in the engine test cell.

Chapter 3

Model of the SI-engine including the EVAP System

In order to be able to simulate the engine and also to be able to develop the method which estimates the mass-flow and mixture of vapours from the EVAP system, a mathematical model of the engine including the EVAP system is needed. In this chapter a *mean-value* model of the engine will be described. The meaning of a ‘mean-value model’ is that variations of physical states within an engine cycle, e.g. engine speed and torque, is treated as mean-values. The model is mainly based on physical relations that have been found to be adequate to describe an SI-engine. Heywood [10], Aquino [1] and Hendricks [8] give a more detailed description of it. Modifications of the model have been done in order to incorporate the EVAP system.

Before the model is described, a short introduction to SI-engines is presented to make the following parts more easy to understand.

3.1 The SI-engine

In Figure 3.1 a principle sketch of an SI-engine is shown. It also includes the purge control valve. Excluded are the turbo-charger and the rest of the EVAP system. When the engine is running, a sub pressure is developed in the intake manifold. Due to the pressure difference over the throttle, air will flow past the throttle into the intake manifold. The air mass-flow \dot{m}_{ath} depends on the intake manifold pressure p_{man} and the throttle plate open area. The air mass-flow is controlled by the throttle angle α , since it determines the throttle plate open area. A closed throttle has $\alpha = 0^\circ$ and a wide open throttle (WOT) has $\alpha = 90^\circ$. Similar to the throttle angle, the PWM control signal u is controlling

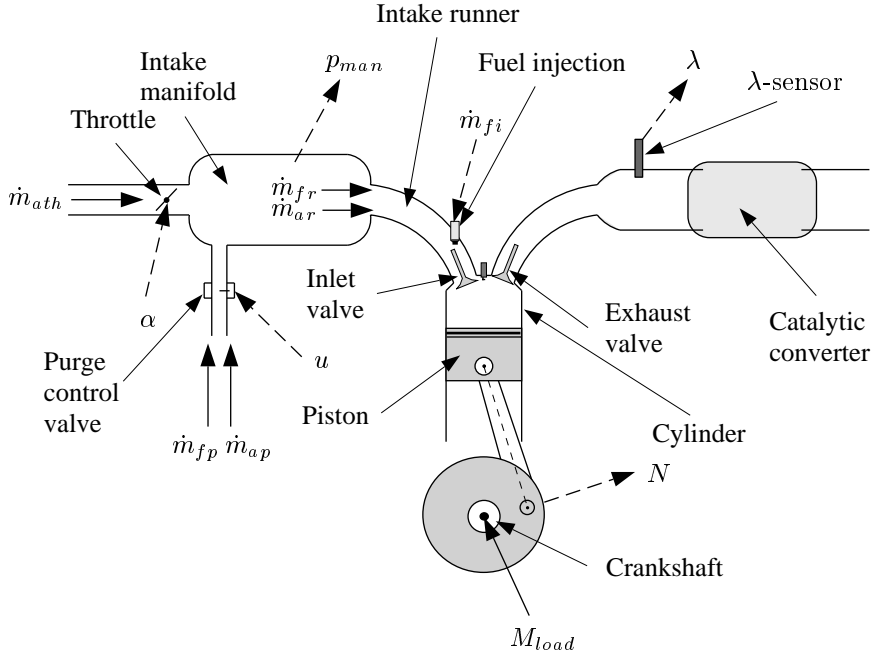


Figure 3.1: Principle sketch of SI-engine.

the vapour flows \dot{m}_{ap} and \dot{m}_{fp} through purge valve. When the inlet valves at the cylinders are open, air \dot{m}_{ar} flows (and also fuel \dot{m}_{fr} from the EVAP system) through the intake runners into the cylinders and are at the same time mixed with injected fuel \dot{m}_{fi} , compressed and ignited to produce a power stroke. The engine to be modeled is a four-stroke engine, i.e. the engine cycle to produce a power stroke is split into four stages.

1. Intake stroke

Starts with the piston at its top position (TC). The inlet valve is open and the exhaust valve closed. While the piston moves downwards it draws fresh air/fuel mixture into the cylinder. When the piston reaches its lowest position (BC), the intake stroke ends.

2. Compression stroke

Both valves are closed and since the piston now moves up towards TC, the mixture inside the cylinder is compressed to a fraction of its initial volume. Just before the piston reaches TC, combustion is initiated by ignition from the spark plug.

3. Power stroke

Keeping both valves closed, the combustion results in a dramatically in-

creased cylinder pressure. The high pressure gases pushes the piston downwards and forces the crankshaft to rotate. The developed work is about five times the work needed to compress the air/fuel mixture. The power stroke ends as the piston reaches BC.

4. Exhaust stroke

The exhaust valve is opened and the burned gases flows out of the cylinder, because the cylinder pressure is initially substantially higher than the exhaust manifold pressure. The piston also pushes the burned gases out of the cylinder as it moves up towards TC to start another four stroke cycle.

During the engine cycle, the crankshaft has rotated 720° .

3.1.1 The Air/Fuel Ratio

As mentioned in Chapter 1, the catalytic converter requires a air/fuel mixture for optimal working capacity. This is also true for the engine, as it is most efficient at stoichiometric air/fuel mixture. Only when maximum power is needed it could be desired to use a rich mixture. i.e. excess fuel is injected. The stoichiometric air/fuel ratio $(A/F)_s$ is fuel dependent and varies between 14.5 and 14.7 for gasoline. In this thesis $(A/F)_s = 14.67$ is assumed. Often used for monitoring the air/fuel ratio (A/F) is the parameter λ , which is defined as the normalized air/fuel ratio

$$\lambda = \frac{(A/F)}{(A/F)_s}$$

or, since $(A/F) = \frac{\dot{m}_{ac}}{\dot{m}_{fc}}$

$$\lambda = \frac{\frac{\dot{m}_{ac}}{\dot{m}_{fc}}}{(A/F)_s} \quad (3.1)$$

$$(3.2)$$

By definition, $\lambda = 1$ for stoichiometric air/fuel mixtures. In modern cars, λ is measured by a λ -sensor. It is mounted before the catalytic converter in the exhaust manifold and measures the excess air in the exhaust gases.

There are two basic types of λ -sensors. The most common type is the *exhaust gas oxygen* (EGO) sensor. The EGO sensor has a sharp relay-like in-out characteristic, thus making it only possible to measure lean ($\lambda > 1$) or rich ($\lambda < 1$) mixtures. The other one, a more expensive type of λ -sensor, the *universal exhaust gas oxygen* (U-EGO) sensor can measure the actual λ and not just lean or rich mixtures. The EGO sensor is sometimes referred to as a discrete λ -sensor and the U-EGO sensor as a continuous λ -sensor.

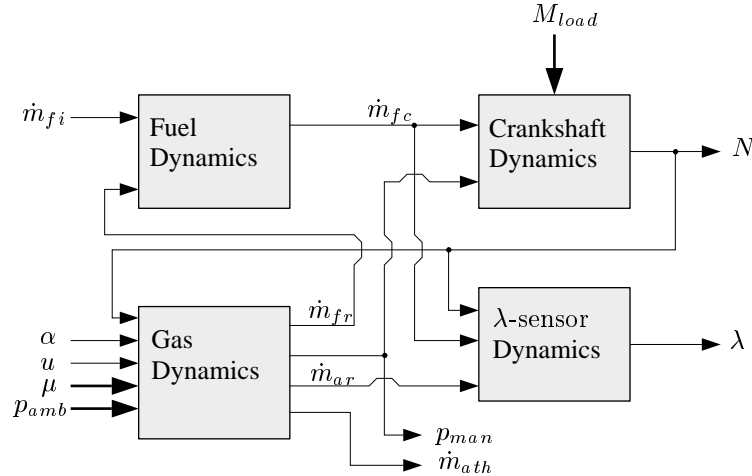


Figure 3.2: Block representation of SI-engine model. Bold arrows represent unknown inputs.

3.1.2 The Structure of the Model

In order to make the modeling more easy, a good idea is to separate the engine into subsystems, which each consists of one or two states. For the engine, three essential subsystems can be identified

1. Gas dynamics
2. Fuel dynamics
3. Crankshaft dynamics

In Figure 3.2, a block model of the engine is illustrated with the different blocks representing the subsystems. A fourth subsystem, representing the λ -sensor dynamics is also shown. Even though the λ -sensor is not really a part of the engine, it influences the engine when it is used for closed loop control of the injected fuel in order to keep λ near 1. Due to that, the λ -sensor is also modeled. Figure 3.2 also gives a feeling of how the different subsystems influences each other.

In the following chapters, gas flows will sometimes be denoted $\dot{n}_{(x)}$ and sometimes be denoted $\dot{m}_{(x)}$. A gas flow denoted $\dot{n}_{(x)}$ means a gas molecule-flow [mole/s] and a gas flow denoted $\dot{m}_{(x)}$ means gas mass-flow [g/s]. Gas mass-flows are for example used in Figure 3.1 and Figure 3.2. To obtain gas mass-flow from gas molecule-flow it have to be multiplied with the molecule weight of the specific gas. The molecule weight of air M_{air} is 28.97 g/mol [13] and the molecule weight of fuel M_{fuel} is between 100-105 g/mol [16]. The

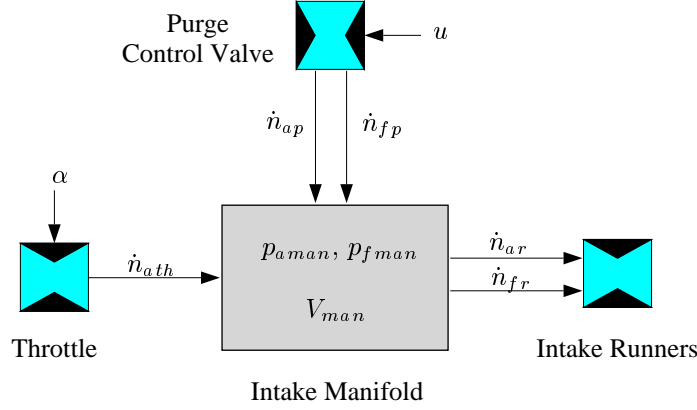


Figure 3.3: A basic block diagram of the intake manifold.

different subscripts stands for type of gas and place of origin. That is a for air and f for fuel, th for throttle, p for purge control valve, r for intake runner and c for cylinder. See also the notations on page iii.

3.2 Gas Dynamics

The gas dynamics in the intake manifold is obtained from the ideal gas law

$$pV = n\tilde{R}T$$

where p is pressure, V volume, n mole number, \tilde{R} the universal gas constant, and T is the temperature. In Figure 3.3, a simplified picture of the intake manifold is shown. The intake manifold is here seen as a volume and the throttle, purge control valve and intake runners, as restrictions of the gas flows. From the ideal gas law, we now obtain the following state space model for the intake manifold pressure

$$\dot{p}_{man} = \frac{\tilde{R}T_{man}}{V_{man}} (\dot{n}_{ath} + \underbrace{\dot{n}_{ap} + \dot{n}_{fp}}_{\dot{n}_p} - \underbrace{\dot{n}_{ar} + \dot{n}_{fr}}_{-\dot{n}_r}) \quad (3.3)$$

The different gas molecule-flows $\dot{n}_{(x)}$ are illustrated in Figure 3.3.

In order to be able to separate fuel from air in the intake manifold, the intake manifold pressure p_{man} is separated into two states, the partial pressure of air p_{aman} and the partial pressure of fuel p_{fman} . That gives a slightly modified

state space model

$$\dot{p}_{aman} = \frac{1}{C}(\dot{n}_{ath} + \dot{n}_{ap} - \dot{n}_{ar}) \quad (3.4)$$

$$\dot{p}_{fman} = \frac{1}{C}(\dot{n}_{fp} - \dot{n}_{fr}) \quad (3.5)$$

$$p_{man} = p_{aman} + p_{fman} \quad (3.6)$$

with

$$C = \frac{V_{man}}{\tilde{R}T_{man}}$$

Under the assumption that the temperature in the intake manifold T_{man} is constant, C will also be constant and it can be seen as the time constant of the intake manifold. No identification of C has been made for this model. Instead a value of C , identified by Åkesson [14] was used.

3.2.1 Air Flow past Throttle

The air molecule-flow past the throttle \dot{n}_{ath} has been shown to be described well by the formula for for a flow through a converging nozzle [15] [10] [13]

$$\dot{n}_{ath}(\alpha, p_{man}) = \frac{C_d(\alpha)A_{th}(\alpha)p_{boost}}{M_{air}\sqrt{R_a T_{man}}} \Psi\left(\frac{p_{man}}{p_{boost}}\right) \quad (3.7)$$

where A_{th} is the throttle plate open area, C_d a discharge coefficient, R_a the specific gas constant for air, and $\Psi\left(\frac{p_{man}}{p_{boost}}\right)$ is

$$\Psi\left(\frac{p_{man}}{p_{boost}}\right) = \begin{cases} \sqrt{\frac{2\kappa}{\kappa-1} \left\{ \left(\frac{p_{man}}{p_{boost}}\right)^{\frac{2}{\kappa}} - \left(\frac{p_{man}}{p_{boost}}\right)^{\frac{\kappa+1}{\kappa}} \right\}} & \text{if } \left(\frac{p_{man}}{p_{boost}}\right) \geq \left(\frac{2}{\kappa+1}\right)^{\frac{\kappa}{\kappa-1}}, \\ \sqrt{\kappa \left(\frac{2}{\kappa+1}\right)^{\frac{\kappa+1}{\kappa-1}}} & \text{otherwise} \end{cases}$$

where $\kappa = \left(\frac{c_p}{c_v}\right)$ is the ratio of specific heats, and p_{boost} the boost pressure before the throttle. Note that the specific gas constant for air $R_a = \frac{\tilde{R}}{M_{air}}$.

Identification and validation of this model was done by Nyberg and Perkovic [15] for the throttle in the SAAB 9-5 engine.

3.2.2 Gas Flow through Purge Control Valve

In an first approach to model the total gas molecule-flow through the purge control valve, the same formula that was used for the throttle, i.e. Equation

(3.7), was applied. It gives the following expression:

$$\begin{aligned}\dot{n}_p(u, p_{man}) &= (\dot{n}_{ap} + \dot{n}_{fp}) = \\ &= \frac{C_d(u)A(u)p_{before}}{M\sqrt{RT}}\Psi\left(\frac{p_{man}}{p_{before}}\right)\end{aligned}\quad (3.8)$$

where $A(u)$ is the open valve area as a function of the PWM control signal u , as well as $C_d(u)$, the discharge coefficient, is a function of u . Note that the pressure before the purge control valve p_{before} must, in order to use this model, be measured.

The molecule weight M , the specific gas constant R , and the ratio of specific heats κ in Equation (3.8) are all dependent of the fuel concentration of the vapours, but the overall dependency of the concentration in (3.8) can be shown to be so small that it might be neglected.

Technical specifications [7] for the purge control valve from the manufacturer supports a model according to Equation (3.8). To identify this physical model an experiment was made when the flow only consisted of air.

The air mass-flow through the purge control valve was measured for ten different manifold pressures and ten different levels of the PWM control signal resulting in a map consisting of 100 nodes. A measurement were made twice for every combination of p_{man} and u and the mean of those two measurements were taken as the value of the node. Since it was not possible to measure the air mass-flow directly with a sensor, the result was obtained by calculating the air mass-flow using an indirect method. The method makes use of relations in the engine that hold for steady state conditions. The method will be further described in Chapter 4.

In Figure 3.4, the measured map is shown together with the best fit of Equation (3.8) to the measurements in a least square sense. A large deviation between the measured map and the physical model can be seen for high manifold pressures and a full open purge control valve. The bad agreement of the measurements to the physical model might indicate that the physics of the purge control valve is not fully known. It is also possible that the measurements are bad.

In order to get a model with better agreement to the measurement, it was decided to use the map as a look-up table instead. The map is then used as a model of the gas molecule-flow through the purge control valve by looking up corresponding values of the gas molecule-flow for the intake manifold pressure and the PWM control signal. When a value of the gas molecule-flow is looked up in the map, interpolation is made between the nodes in order to be able to get values not corresponding to any node. The map can be seen as a function with as many parameters as there are nodes

$$\dot{n}_p(u, p_{man}) = f(u, p_{man}) \quad (3.9)$$

The advantage of using a map is that it gives a very good model over an unknown static system. The disadvantages are that it gives no physical

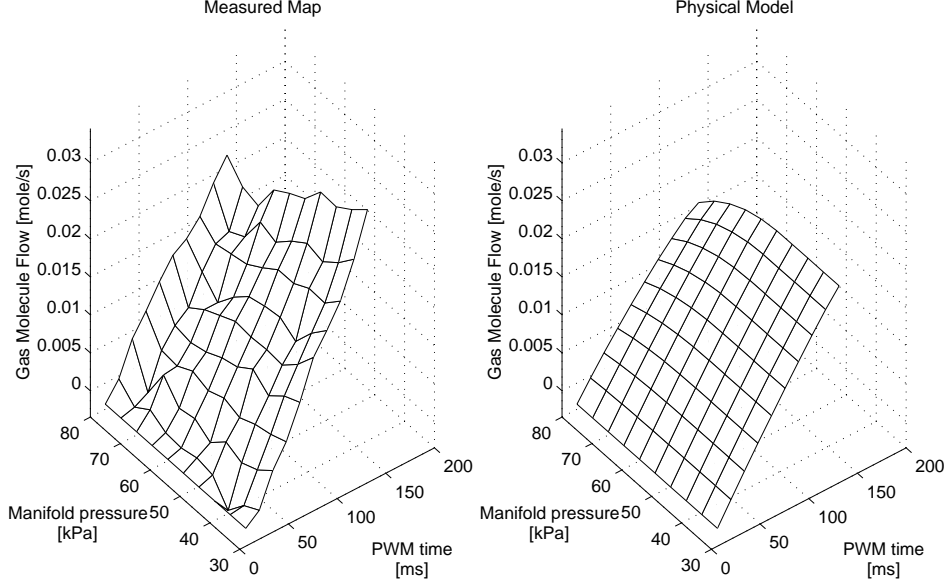


Figure 3.4: Map of the molecule-flow through the purge control valve together with the best fit of the physical model to the measurement.

understanding of the system and it uses large number of parameters. By using a physical model as the one in Equation (3.8), the parameters becomes few and there will be a physical understanding of the system.

The function (3.9) only describes the total gas molecule-flow \dot{n}_p through the purge control valve. In order to extract the part of fuel and the part of air in the flow, the mass concentration μ of fuel in the vapours will be introduced. The mass concentration μ can be written as

$$\mu = \frac{\dot{m}_{fp}}{\dot{m}_{fp} + \dot{m}_{ap}} = \frac{M_{fuel}\dot{n}_{fp}}{M_{fuel}\dot{n}_{fp} + M_{air}\dot{n}_{ap}} \quad (3.10)$$

and since

$$\dot{n}_p = \dot{n}_{fp} + \dot{n}_{ap}$$

it gives that

$$\dot{n}_{fp} = \frac{\mu M_{air}}{(1 - \mu)M_{fuel} + \mu M_{air}} \dot{n}_p \quad (3.11)$$

$$\dot{n}_{ap} = \frac{(1 - \mu)M_{fuel}}{(1 - \mu)M_{fuel} + \mu M_{air}} \dot{n}_p \quad (3.12)$$

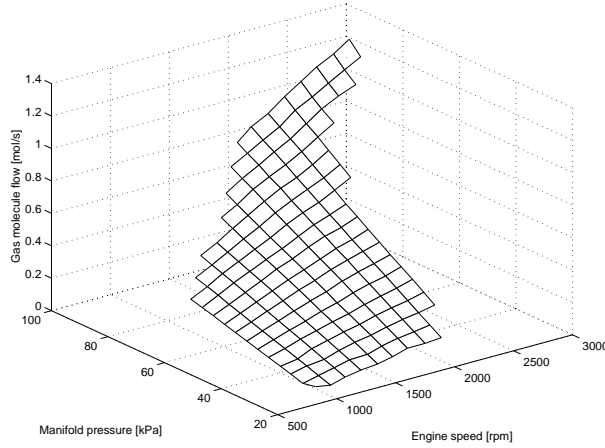


Figure 3.5: The gas molecule-flow through the intake runners as function of engine speed and intake manifold pressure.

3.2.3 Gas Flow through Intake Runners

Since there is no accurate and simple physical model describing the gas molecule-flow through the intake runners, a map is used here also. In Figure 3.5 the map is shown. The map describes the total gas molecule-flow as a function of manifold pressure p_{man} and engine speed N

$$\dot{n}_r(N, p_{man}) = \dot{n}_{ar} + \dot{n}_{fr} = g(N, p_{man}) \quad (3.13)$$

The concentration of fuel in the gas molecule-flow in the intake runners is assumed to be equal to the concentration of fuel in the intake manifold. The concentration can be described by the partial pressures of fuel and air in the intake manifold which gives

$$\dot{n}_{fr} = \frac{p_{fman}}{p_{fman} + p_{aman}} \dot{n}_r \quad (3.14)$$

$$\dot{n}_{ar} = \frac{p_{aman}}{p_{fman} + p_{aman}} \dot{n}_r \quad (3.15)$$

Since the air flow through the intake runners is the only air that enters the cylinders we also have

$$\dot{n}_{ac} = \dot{n}_{ar} \quad (3.16)$$

The map was constructed by Nyberg and Perkovic [15] for air mass-flow through the intake runners of the SAAB 9-5 engine. By dividing it with the molecule weight of air M_{air} , the gas molecule-flow through the intake runners is given.

3.3 Fuel Dynamics

When fuel is injected, it is injected short before the intake valve in the intake runners. Most of the fuel injected is drawn directly as liquid into the engine but a considerable part strikes the inside wall of the intake manifold and creates a liquid film there. The liquid film can be seen as a puddle of fuel where some part of the fuel injected adheres. From the puddle, fuel also evaporates. A model of the first order is used to describe the dynamics of the puddle [1]

$$\dot{m}_{puddle} = X\dot{m}_{fi} - \frac{m_{puddle}}{\tau_f} \quad (3.17)$$

where the first term on the right hand side describes the part of the injected fuel that adheres to the puddle and the second part describes the evaporation from the puddle. The fuel mass-flow into the cylinders is now given by

$$\dot{m}_{fc} = \dot{m}_{fi} - \dot{m}_{puddle} + \dot{m}_{fr} = (1 - X)\dot{m}_{fi} + \frac{m_{puddle}}{\tau_f} + \dot{m}_{fr} \quad (3.18)$$

This model is known to give a good qualitative model of the fuel dynamics [10] [1]. The parameters X and τ_f is treated as constants here, but in reality they depend on the engine speed N , the temperature T_{man} and the intake manifold pressure p_{man} . As seen in (3.18), the additional fuel flow \dot{m}_{fr} that originates from the EVAP system comes in as a direct term here. It is assumed that this additional fuel flow not influences the puddle even though that might not be completely true.

No identification of X and τ_f in this model has been made. Values of X and τ_f used in similar studies by Åkesson [14] is used here.

3.4 Crankshaft Dynamics

The crankshaft is modeled according to Newton's Second Law for rotating masses. It can be stated as

$$M = J\dot{\omega} \quad (3.19)$$

where M is the total torque acting upon the rotating mass, ω the angular velocity and J the moment of inertia. For the crankshaft, the equation becomes

$$J \frac{2\pi}{60} \dot{N} = M_{in} - M_{friction} - M_{load} \quad (3.20)$$

$$M_{in} = \frac{\eta_f Q_{HV} \dot{m}_{fc} (t - t_c)}{\frac{2\pi}{60} N} \quad (3.21)$$

$$M_{friction} = a_0 + a_1 N + a_2 N^2 + (a_3 + a_4 N) p_{man} \quad (3.22)$$

where M_{in} is the torque created by the power stroke, $M_{friction}$ the loss in torque due to engine friction and M_{load} the load torque from the transmission in a real car or, as in the test cell, the counteracting torque from the dynamometer. Further, η_f is the fuel conversion efficiency, which is a measure of the engine's efficiency and is defined as

$$\eta_f = \frac{P}{\dot{m}_{fc} Q_{HV}} \quad (3.23)$$

where P is the output power. Here η_f is seen as a constant but it is usually seen as dependent on λ , N and p_{man} . Moreover, Q_{HV} is the heating value of the fuel, that is the heat released per kilogram fuel when combusted. For gasoline this value is between 42 and 44 MJ/kg [10]. In this thesis 43 MJ/kg has been used as value of Q_{HV} . The time delay t_c of the fuel in Equation (3.21) comes from the fact that the crankshaft has to rotate 360° before the fuel is ignited, i.e. $t_c = \frac{60}{N}$. Note that the relation $\omega = \frac{2\pi}{60}N$ has been used in (3.20) and (3.21).

A physical model for the friction loss in (3.22) is not known and therefore a parametric model is used. Values for the parameters in (3.22) and also η_f and J has not been identified. They have also been taken from similar studies by Åkesson [14].

3.5 λ -sensor Dynamics

For all measurement systems, one desire that a sensor is fast compared to the system it monitors. If the sensor is fast, its dynamics can usually be neglected when modeling the system. In the case of the λ -sensors used in cars, this is not the case. First, the λ -sensor is usually mounted some decimeters away from the exhaust valve, giving a pure time delay t_d in the measurement which depends on the speed of the exhaust gases, which secondly depends on the engine speed N , but also a little on the exhaust manifold pressure. Second, the sensor response is somewhat slower than the dynamics of the gases in the exhaust manifold. As it is, the λ -sensor has to be modeled too. A first order model of the sensor can be described as

$$\dot{\lambda}_{meas} = \frac{1}{\tau_\lambda}(\lambda(t - t_d) - \lambda_{meas}) \quad (3.24)$$

where λ_{meas} is the measured value and λ , according to (3.1), is

$$\lambda = \frac{\dot{m}_{ac}}{(A/F)_s \dot{m}_{fc}}$$

and with time delay t_d

$$t_d = \frac{k}{N} \quad (3.25)$$

In the case of a EGO sensor the output will be

$$v = \begin{cases} 1 & \text{if } \lambda_{meas} < 1, \\ 0 & \text{if } \lambda_{meas} > 1 \end{cases} \quad (3.26)$$

No identification of the parameters τ_λ and k in the model has been made. Here also values of τ_λ and k has been taken from similar studies by Åkesson [14].

Chapter 4

Gas Flow Estimation Method

Since the normal closed loop λ -control can not handle the large quantities of fuel vapour that originates from the EVAP system most cars equipped with an EVAP system opens the purge control valve very carefully. The λ -controller may be able too handle this, but its performance will not be improved. By open the purge control valve carefully it is also not possible to purge the canister aggressively either, so that the canister could be emptied each time the car is used. If, on the other hand, estimates of the vapour flow that originates from the EVAP system where at hand, compensation for them could be done before the closed loop λ -controller corrects the injected fuel in a fuel calculation algorithm. By doing so, the λ -controller will only correct for small changes of λ from 1, as it is constructed for.

In this chapter will a method estimating the fuel mass-flow \dot{m}_{fr} and the total air mass-flow \dot{m}_{ar} through the intake runners be presented. The method is based on some of the models described in Chapter 3. The method makes no use of extra sensors. For many car companies, extra sensors is not desirable because they give more sensors that can go bad and has to be monitored in a diagnostic system. In that point of view the method is also preferable.

The companies behind the EVAP system used in this thesis, GM and Delphi-Energy and Engine Management Systems have in a paper [6] proposed a slightly different approach to estimate the vapour flow. They make use of two extra sensors. One sensor measures the pressure before the purge control valve. The other one is an acoustical sensor which can measure the concentration in the fuel vapour line from the canister. They also make use of the physical model over the purge control valve discussed in Section 3.2.2.

4.1 Estimation of Gas Flow from the EVAP System

The amount of gas flow through the purge control valve into the intake manifold can be established by using the model for the intake manifold gas dynamics from Equation (3.3) in an observer of the intake manifold pressure. An observer of the intake manifold pressure \hat{p}_{man} can be expressed as

$$\begin{aligned} \dot{\hat{p}}_{man} = & \frac{1}{C}(\dot{n}_{ath}(\alpha, \hat{p}_{man}) + \dot{n}_p(u, \hat{p}_{man}) - \dot{n}_r(N, \hat{p}_{man})) \\ & + K(p_{man} - \hat{p}_{man}) \end{aligned} \quad (4.1)$$

where the models of the throttle \dot{n}_{ath} (3.7), purge control valve \dot{n}_p (3.9) and gas flow through the intake runners \dot{n}_r (3.13) has been incorporated. In the observer (4.1), K is a constant greater than zero. The value of K is a choice between noise reduction and accuracy in the observer. If a small value of K is used, the observer relies much on the model's accuracy and noise from the measured value is reduced. On the other hand if a big value of K is used, the model does not have to be so accurate, but there will also be little noise reduction.

The outputs from the observer is chosen to be $\dot{n}_p(u, \hat{p}_{man})$ and $\dot{n}_r(N, \hat{p}_{man})$. They will from now on be denoted \hat{n}_p and \hat{n}_r to show that they are estimates. In order to account for the effect that \hat{n}_p is transported through the intake manifold, a low pass filter

$$H(s) = \frac{5.5}{s + 5.5} \quad (4.2)$$

is used as a simplified model of the intake manifold dynamics which gives

$$\hat{n}_{pr} = H(p)\hat{n}_p \quad (4.3)$$

where $H(p)$ denotes the transfer operator of the filter $H(s)$. The coefficients has been chosen to give the filter dynamics close to the dynamics of the intake manifold. Since the dynamics of the intake manifold is included in the observer (4.1), the question arise why $H(s)$ in (4.2) is needed. It is needed because it was not found possible to extract \hat{n}_{pr} from the observer (4.1). Maybe it is possible, but as said above that solution was not found.

If the concentration of fuel in the gas flow μ was known, an estimate of \dot{n}_{fr} could be established. Now assume that an estimate of μ , i.e. $\hat{\mu}$ is known. Then use $\hat{\mu}$ and the relation (3.11) to calculate \hat{n}_{fr} as follows

$$\hat{n}_{fr} = \frac{\hat{\mu}M_{air}}{(1 - \hat{\mu})M_{fuel} + \hat{\mu}M_{air}}\hat{n}_{pr} \quad (4.4)$$

The desired estimates are then given by

$$\hat{m}_{fr} = M_{fuel} \hat{n}_{fr} \quad (4.5)$$

$$\hat{m}_{ar} = M_{air}(\hat{n}_r - \hat{n}_{fr}) \quad (4.6)$$

So by using (4.1), (4.3) and (4.4) and assuming that an estimate of μ is known, it has now been shown that the estimates \hat{n}_{fr} and \hat{n}_{ar} can be established. They can now be used for compensation in a fuel calculation algorithm.

4.2 Derivation of Steady State Relations

As seen from the previous section an estimate of the concentration μ in the vapour flow is needed. An estimate of μ can be established by using relations that hold under steady state conditions. These relations will be derived here. From the definition of λ in (3.1) we have that

$$M_{air} \dot{n}_{ac} = \lambda(A/F)_s M_{fuel} \dot{n}_{fc} \quad (4.7)$$

and under steady state conditions it holds that

$$\dot{n}_{fc} = \dot{n}_{fi} + \dot{n}_{fr} = \dot{n}_{fi} + \dot{n}_{fp} \quad (4.8)$$

$$\dot{n}_{pr} = \dot{n}_p = \dot{n}_{ap} + \dot{n}_{fp} \quad (4.9)$$

where both manifold dynamics and fuel dynamics are neglected. Since

$$\dot{n}_{ac} = \dot{n}_{ar} = \dot{n}_r - \dot{n}_{fr} \quad (4.10)$$

we can substitute (4.8) and (4.10) into (4.7) and get

$$M_{air}(\dot{n}_r - \dot{n}_{fr}) = \lambda(A/F)_s M_{fuel}(\dot{n}_{fi} + \dot{n}_{fr})$$

which implies

$$\lambda(A/F)_s M_{fuel} \dot{n}_{fr} + M_{air} \dot{n}_{fr} = M_{air} \dot{n}_r - \lambda(A/F)_s M_{fuel} \dot{n}_{fi}$$

and finally get

$$\dot{n}_{fr} = \frac{M_{air} \dot{n}_r - \lambda(A/F)_s M_{fuel} \dot{n}_{fi}}{\lambda(A/F)_s M_{fuel} + M_{air}} \quad (4.11)$$

Now by using (4.8) and (4.9) in the definition of μ (3.10), μ can be rewritten as

$$\mu = \frac{M_{fuel} \dot{n}_{fr}}{M_{fuel} \dot{n}_{fr} + M_{air}(\dot{n}_{pr} - \dot{n}_{fr})} \quad (4.12)$$

In the measurement described in Chapter 3 relation (4.7) and

$$\begin{aligned}\dot{n}_{ac} &= \dot{n}_{ar} = \dot{n}_{ath} + \dot{n}_{ap} \\ \dot{n}_{fc} &= \dot{n}_{fi}\end{aligned}$$

are used, which hold under steady state conditions and when the vapour flow only contains air. They give the flow through purge control valve as follows

$$\dot{n}_p = \dot{n}_{ap} = \frac{\lambda(A/F)_s M_{fuel} \dot{n}_{fi}}{M_{air}} - \dot{n}_{ath} \quad (4.13)$$

In Chapter 6 relation (4.8), (4.9), (4.11) and (4.12) will be used to calculate the fuel mass-flow, air mass-flow and mass concentration in the measurements described there.

4.3 Estimation of Concentration in the Vapour Flow

The estimate of μ needed in (4.4) can now be derived by using relations (4.11) and (4.12). From (4.11) a second estimate of \dot{n}_{fr} can be done

$$\hat{\dot{n}}_{fr} = \frac{M_{air} \hat{\dot{n}}_r - \lambda_{meas}(A/F)_s M_{fuel} \dot{n}_{fi}}{\lambda_{meas}(A/F)_s M_{fuel} + M_{air}} \quad (4.14)$$

and μ can be estimated according to (4.12)

$$\mu_{est} = \frac{M_{fuel} \hat{\dot{n}}_{fr}}{(M_{fuel} - M_{air}) \hat{\dot{n}}_{fr} + M_{air} \hat{\dot{n}}_{pr}} \quad (4.15)$$

where $\hat{\dot{n}}_{pr}$ was derived in Equation (4.3).

Since the relation used to calculate μ_{est} only is valid under steady state conditions it takes some time for the estimations to stabilize. It can also be shown that an algebraic loop is established for \dot{n}_{fi} if μ_{est} is used in (4.4) in a fuel calculation algorithm. This can be solved by using a special kind of observer for μ_{est} . The observer brakes the algebraic loop and it also stabilizes μ_{est} as it works as low pass filter. The observer can be written as

$$\dot{\hat{\mu}} = \begin{cases} K_\mu (\mu_{est} - \hat{\mu}) & \text{if } u > 0 \\ 0 & \text{if } u = 0 \end{cases} \quad (4.16)$$

where K_μ is a constant which has to be trimmed when the method is implemented in a fuel control algorithm and validated. The observer has another feature. As shown in (4.16) the observer is shut off then the purge control valve is closed. This makes the observer to remain its value until the purge control

valve is opened again. This will be shown in Chapter 7 to be very useful if the purge control valve has to be closed and opened in short intervals.

Now by using (4.16) in (4.4) estimations of \dot{m}_{fr} and \dot{m}_{ar} according to (4.5) and (4.6) can be made and compensations are possible in a fuel control algorithm.

Chapter 5

Fuel Control Algorithm

A fuel control algorithm based on both an open loop control algorithm and a closed loop control algorithm, will here be described. In Figure 5.1 the algorithm is illustrated. The open loop algorithm uses the method to estimate the gas flows through the intake runners described in the previous chapter. The closed loop algorithm is a standard λ -controller.

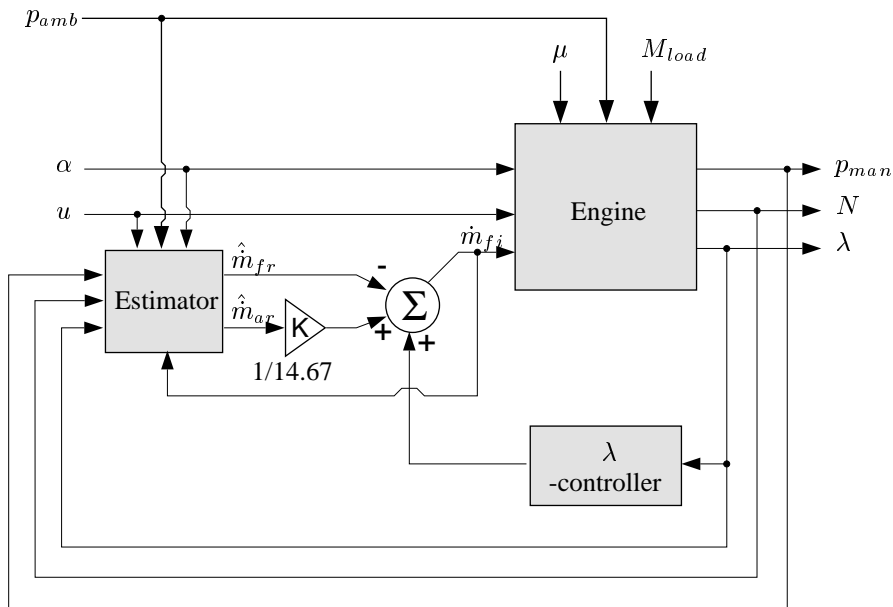


Figure 5.1: Illustration of fuel control algorithm.

The estimates \hat{m}_{fr} and \hat{m}_{ar} are calculated according to the estimation method (4.5) (4.6) in Chapter 4. As inputs it uses the intake manifold pressure p_{man} , the engine speed N , the purge control signal u , the throttle angle α , the ambient pressure p_{amb} and, if a continuous λ -sensor is used, a measure of λ . In the case of a discrete λ -sensor it is assumed that λ is near 1 and 1 replaces λ_{meas} in (4.14). The estimated air mass-flow \hat{m}_{ar} divided by the stoichiometric air/fuel ratio $(A/F)_s$ then gives the required fuel mass-flow to be injected. To compensate for the extra fuel flow, \hat{m}_{fr} is subtracted from the required fuel mass-flow. Finally, unknown factors making λ to deviate from 1, the closed loop λ -control makes corrections for. It is done by adding the output from the λ -controller as correction factor to the required fuel mass-flow. In algebraic form the algorithm becomes

$$\dot{m}_{fi} = \frac{1}{(A/F)_s} \hat{m}_{ar} - \hat{m}_{fr} + d_\lambda \quad (5.1)$$

The λ -controller is a standard PI-controller

$$d_\lambda = K_p(1 - \lambda_{meas}) + K_i \int (1 - \lambda_{meas}) dt \quad (5.2)$$

In the case of a discrete λ -sensor the output from the sensor is transformed to a variable which is -1 for $\lambda_{meas} < 1$ and 1 for $\lambda_{meas} > 1$. This variable then replaces $(1 - \lambda_{meas})$ in (5.2).

Chapter 6

Carbon Canister

To get a broader understanding of the EVAP system, the physics behind the carbon canister and an approach to model it will be presented in this chapter. Further work to get a model over the carbon canister good enough for simulations is also interesting because it may be possible to use the estimated concentration in the vapour flow to decide the amount of fuel in the carbon canister. Together with a model of the evaporation of fuel from the fuel tank it could for example be used to alarm the owner of the car that the canister is full and also to command the purge control valve to shut when the canister is emptied.

6.1 Adsorption and Activated Carbon

The most important process in the EVAP system is the *adsorption* process in the carbon canister, which makes it possible to trap fuel vapour there. Here will a theoretical orientation on adsorption and some words about *activated carbon* be presented.

During adsorption, one or more fluid components are removed from a fluid by adhering to the surface of a solid. This is in contrast to *absorption*, where one matter diffuse into the structure of another matter. The fluid molecules being removed by adsorption are referred to as the *adsorbate*, while the solid doing the adsorbing is called the *adsorbent*.

Adsorption is an extremely complex thermochemical process that is not fully understood. The attractive forces which hold the fluid to the surface of the solid are electrostatic in nature. The adsorption process is an *exothermic*¹ process and is either physical or chemical in nature. The basic difference between *physical adsorption* and *chemical adsorption* is the manner in which the adsorbate is bonded to the the adsorbent. Physical adsorbtion uses weak

¹A process that releases heat.

van der Waals' forces and the chemical nature of the adsorbate remains unchanged. Chemical adsorption uses stronger forces and a sharing or exchange of electrons takes place. The *enthalpy*² of physical adsorption is of the same order as the enthalpy of condensation, while the enthalpy of chemical adsorption is of the same order as the enthalpy of the corresponding chemical reaction. Chemical adsorption will not be discussed further, since it does not occur in the carbon canister.

6.1.1 Physical Adsorption

Physical adsorption can occur from three different effects: an *orientation effect*, a *dispersion effect* or an *induction effect*, see Figure 6.1. In the left picture in Figure 6.1 polar molecules are attracted to a polar surface because of the orientation effect. The negative area of a polar molecule will be oriented towards a positive area of the polar surface.

Nonpolar molecules are attracted to a nonpolar surface because of the dispersion effect, the middle picture in Figure 6.1. Although nonpolar substances do not have a permanent dipole they do have fluctuating or oscillating dipoles. When two nonpolar molecules come close to one another they can fluctuate in phase with each other and their total energy decreases. Oscillating dipoles disperse light, thereby the name dispersion effect.

A polar molecule can attract a nonpolar molecule by induction - the induction effect, the right picture in Figure 6.1. The induction effect is very small compared to the orientation and dispersion effect, and is often neglected. Therefore adsorption systems use polar adsorbents to remove polar substances, e.g. water vapour and nonpolar adsorbents to remove nonpolar substances, e.g. organic fluids [12].

The nature of the adsorption that occurs in the carbon canister is physical adsorption of a gas and from here on, the discussion concerns gas-phase physical adsorption even if it might be valid for adsorption of liquids too. Gas-phase physical adsorption will from here on be called just adsorption also. Both fuel vapours and activated carbon are nonpolar so the adsorption in the carbon canister occurs due to the dispersion effect. Activated carbon is just pure carbon with an increased surface area. That is made by increasing the pore structure of the carbon. The surface area of activated carbon can range from 500 to 1500 m²/g [9].

6.1.2 Isotherms

An adsorption process will eventually reach a point of equilibrium, where the rate of molecules being adsorbed is equal to the rate of molecules being *desorbed*³.

²The heat uptaken or released from a process under constant pressure [2].

³Desorption is the opposite process of adsorption, but can also be used as the opposite process of absorption.

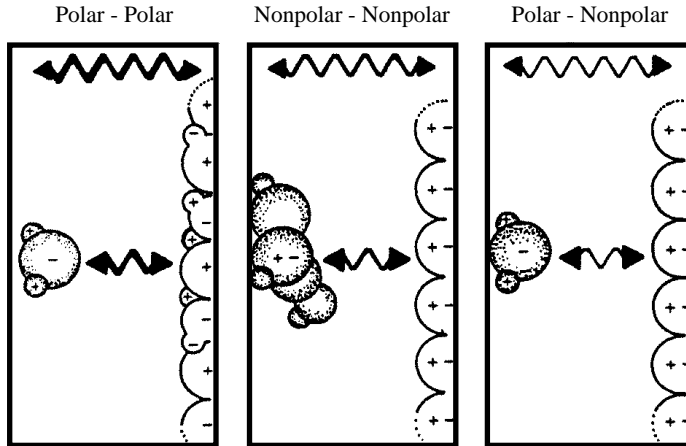


Figure 6.1: Physical forces causing adsorption. Left - the orientation effect. Middle - the dispersion effect. Right - the induction effect.

This is often described as an *isotherm*⁴. In Figure 6.2, the five basic types of adsorption isotherms are illustrated [3]. The amount (mass) adsorbed gas in equilibrium is plotted as a function of the partial pressure of the gas in equilibrium. Over the saturation vapour pressure (p_s) the gas starts to condense and the isotherm is of no interest anymore. The most common isotherms are of Type I. Usually one has to determine the isotherm experimentally and then adapt a mathematical function to the data. Often it is not so essential what kind of mathematical function one uses.

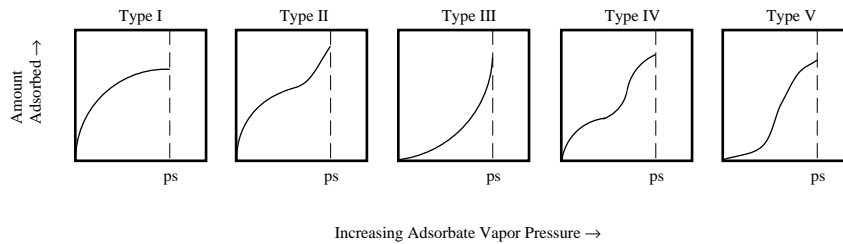


Figure 6.2: The five basic types of adsorption isotherms. p_s = Saturation vapour pressure.

⁴From the Greek words for 'equal heat' and means a relation, often plotted, between some physical variables under constant temperature.

6.1.3 Dynamic Adsorption and Concentration Profiles

The equilibrium is by itself not sufficient to describe the adsorption process when there is a moving gas stream present. One way to describe a dynamic adsorption or desorption process is to plot how the concentration of the fluid varies with time at the outlet of the adsorbent bed or as function of a coordinate axis through the adsorbent bed at a fixed time. It can look like Figure 6.3 for adsorption.

It has been seen from many experiments that during adsorption a saturated zone will build up and move through the carbon bed, with near constant speed v' . The speed v' depends on the velocity of the stream and the amount of activated carbon available for the stream. Saturated zone means that the equilibrium of adsorption is reached in that zone. Within the zone, the concentration is at constant maximum level. Figure 6.3 and Figure 6.4 illustrates this constant maximum concentration level. For desorption, i.e. when the canister is *regenerated*, the plot is flipped as in Figure 6.4. Regeneration of the canister means that the canister is purged from fuel by the engine, in order to be able to use the canister again.

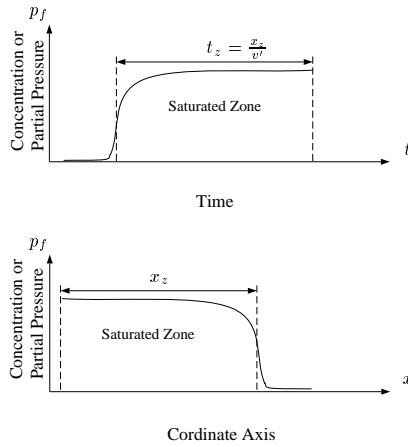


Figure 6.3: Concentration profile during adsorption. The upper figure shows a concentration profile over time at the outlet of the adsorption bed. The lower figure shows a concentration profile as function of an axis through the adsorption bed. The direction of the flow in the lower figure is in the direction of the coordinate axis.

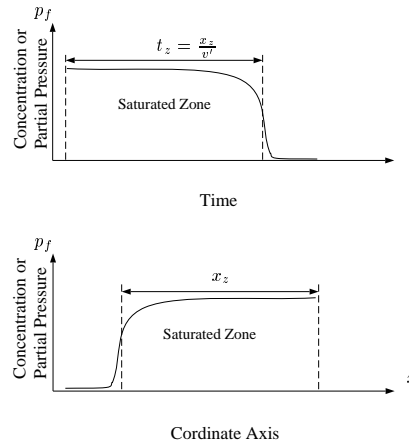


Figure 6.4: Concentration profile during desorption. The upper figure shows a concentration profile over time at the outlet of the adsorption bed. The lower figure shows a concentration profile as function of an axis through the adsorption bed. The direction of the flow in the lower figure is in the direction of the coordinate axis.

6.2 Analytical Approach to Model the Canister

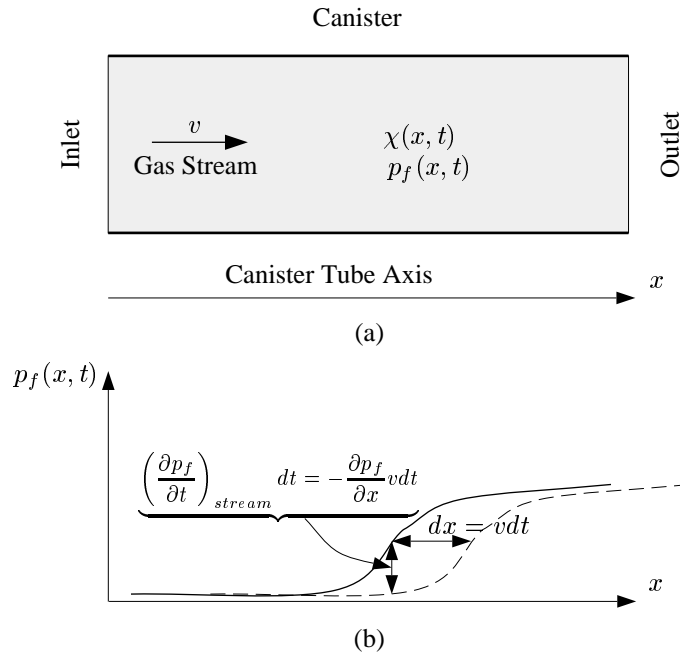


Figure 6.5: (a) A simplified picture of the canister. In the lower figure (b) it is showed how the movement of the partial pressure profile influences $\frac{\partial p_f}{\partial t}$.

A simplified picture of the canister can be seen as a tube filled with activated carbon, see Figure 6.5a. Assuming that the canister is regenerated, a stream of air with velocity v is regenerating the canister. The concentration χ [mole/m³] of fuel adsorbed on the activated carbon and the partial pressure of fuel vapours p_f in the canister are assumed to be constant along a cross-section of the canister. Further, χ and p_f are assumed to be varying with time t and along an axis x through the canister tube. Since χ is just another measure of the amount adsorbed and since the adsorption is driven against an equilibrium of the amount adsorbed and the partial pressure, it can be assumed that the rate of change of χ , i.e. $\frac{\partial \chi}{\partial t}$, in a cross-section of the canister is a function of χ and p_f

$$\frac{\partial \chi}{\partial t} = f(\chi, p_f) \quad (6.1)$$

Under these assumptions, a relation of p_f expressed as a partial differential

equation will here be derived. The derivative of p_f with respect to time is

$$\frac{dp_f}{dt} = \frac{\partial p_f}{\partial t} + \frac{\partial p_f}{\partial x} \dot{x} \quad (6.2)$$

according to the chain rule. It can be seen as the change-rate of p_f that an observer “sees” if he is traveling with velocity \dot{x} through the canister. If the observer fixes his position, he will only observe $\frac{\partial p_f}{\partial t}$, the explicit time dependence in p_f and when moving, an additional change will occur due to the slope of the partial pressure profile and the velocity.

Now consider a fix position in the canister, corresponding to $\frac{\partial p_f}{\partial t}$ in (6.2). Since both adsorption and movement caused by the stream is present for the fuel vapour, $\frac{\partial p_f}{\partial t}$ can be seen as consisting of two parts, one part due to adsorption as if no stream were present and another part due to movement of the stream as if no adsorption were present. That is

$$\frac{\partial p_f}{\partial t} = \left(\frac{\partial p_f}{\partial t} \right)_{adsorption} + \left(\frac{\partial p_f}{\partial t} \right)_{stream} \quad (6.3)$$

First look at the adsorption part of (6.3). A positive change in the partial pressure Δp_f corresponds to a negative change in the concentration of adsorbed fuel $\Delta \chi$. The relation between p_f and the concentration of the surrounding fuel vapours c_f [mole/m³], is according to the Ideal Gas Law

$$p_f = c_f \tilde{R}T$$

where \tilde{R} is the universal gas constant and T is the temperature. Since $\Delta \chi = -\Delta c_f$ we can write the adsorption part of (6.3) as

$$\left(\frac{\partial p_f}{\partial t} \right)_{adsorption} = -\frac{\partial \chi}{\partial t} \tilde{R}T = -f(\chi, p_f) \tilde{R}T \quad (6.4)$$

Now consider the part of (6.3) due to the stream. If no adsorption is present, the observer mentioned earlier will see no change in p_f when moving with the same velocity v as the stream (no concern is taken to turbulence in the stream). An illustration is shown in Figure 6.5b to explain this. It can be expressed with (6.2) as

$$\frac{dp_f}{dt} = \left(\frac{\partial p_f}{\partial t} \right)_{stream} + \frac{\partial p_f}{\partial x} v = 0$$

which implies

$$\left(\frac{\partial p_f}{\partial t} \right)_{stream} = -\frac{\partial p_f}{\partial x} v \quad (6.5)$$

By substituting (6.4) and (6.5) into (6.3) it gives that

$$\frac{\partial p_f}{\partial t} = -f(\chi, p_f)\tilde{R}T - \frac{\partial p_f}{\partial x}v \quad (6.6)$$

In a paper by I. Neretnieks, P-J Aronson and M. Westermark [11] an equation for a stationary adsorption bed is presented which says that, with variables renamed to fit this thesis

$$\frac{\partial p_f}{\partial t} + f(\chi, p_f)\tilde{R}T + \frac{\partial p_f}{\partial x}v = D\frac{\partial^2 p_f}{\partial x^2} \quad (6.7)$$

The only differences between (6.6) and (6.7) are the second order derivative and the constant D in (6.7). They stand for the dispersion of fuel vapour due to the concentration differences along the axis through the canister tube. If that is a big or small effect has not been investigated here.

Equation (6.6) can be connected to what was said in Section 6.1.3 about saturated zones moving with near constant speed v' through the canister. If it shows that $\frac{\partial p_f}{\partial t}$ can be expressed as

$$\frac{\partial p_f}{\partial t} = -f(\chi, p_f)\tilde{R}T - \frac{\partial p_f}{\partial x}v = -\frac{\partial p_f}{\partial x}v'$$

it follows that

$$\frac{dp_f}{dt} = -\frac{\partial p_f}{\partial x}v' + \frac{\partial p_f}{\partial x}v' = 0$$

That is, if the observer is moving with the same speed v' as the saturated zone he will not experience any change of p_f .

To solve (6.6) some sort of Finite Element Method could be used. Since the objective here was just to understand how the carbon canister works, (6.6) was not solved. It was found adequate if a concentration profile could be measured from the canister and compared with the empirical one in Figure 6.4. This measurement will be presented in the next section.

6.3 Measurement on the Carbon Canister

In this section measurements made on the carbon canister will be described. A concentration profile will be calculated from the measurements and other measurements of the mass loss of the canister will be compared with calculation of the fuel mass-flow from the canister.

Because no equipment for measuring the mass flows from the canister was available an indirect measurement method was used. The method was explained briefly in Chapter 4. First, assume that the flows can be measured directly.

By measuring the mass flow of air \dot{m}_{ap} and fuel \dot{m}_{fp} from the canister, a mass concentration profile $\mu(t)$ can be achieved. Integrating the mass flow of

fuel also gives the mass loss of the canister and if the mass of fuel in the canister is known at the beginning of the measurement, the change in fuel mass can be monitored.

To draw the fuel out of the canister, the engine was used just as it is done under normal operation of the EVAP system. Since no sensors were available for direct measurement of \dot{m}_{ap} and \dot{m}_{fp} , the indirect method was used.

6.3.1 Preparation and Setup of Measurement

First the canister had to be prepared for the experiment. The canister was weighed empty on an electric scale. Then under several weeks the canister was connected to the fuel tank in order to load up evaporated fuel. The long time for charging the canister comes from the fact that the temperature in the test cell is only around 17 °C. It is a little bit too low for the gasoline to evaporate quickly. It was decided to speed up the process a little bit in order to achieve an almost full canister. By heating gasoline in a spare tank with hot water to a temperature of 30-35 °C and with the canister connected to the spare tank, almost as much fuel adsorbed as it had done during the previous weeks. However the canister was not full yet; it was just a little more than half full but it was decided to proceed with the experiment. From technical specifications [5] of the canister from the manufacturer it has been estimated that a full canister should have gained around 260 g of fuel. Here the canister has only gained 153 g.

During the experiment, the engine was held at constant speed 1500 rpm and constant intake manifold pressure 40 kPa. The canister was weighed on the electric scale just before the experiment and then every 19.5 minute, the engine was stopped and the canister was weighed again. Measured parameters is presented in Table 6.1. Some parameters were never used in the further calculations but were measured to be able to monitor possible misbehavior during the experiment.

Since the engine was held at steady state, the gas flow through the intake runners equals the gas flow past the throttle when the purge control valve is closed. A short time before the purge control valve was opened and a short time after the valve was closed again measurements of the gas flow through the intake runners \dot{n}_r was made by measuring the flow past the throttle with the air mass meter. When the purge control valve is opened the gas flow through the intake runners will not change since the intake manifold pressure p_{man} and the engine speed N are held constant.

The air mass meter in the engine is not so accurate. In order to get the best performance of the experiment, a mean value of the measures from the air mass meter when the purge control valve was closed, were taken as the value of \dot{n}_r for the whole experiment. The air mass meter also had a bias that had to be added to \dot{n}_r in order to get a more correct value of \dot{n}_r .

A special program from SAAB Automobile AB collected the data from Trionic T7. The PWM control signal u was controlled from Matlab via Trionic

Trionic T7	Additional Sensors
\dot{m}_{ath}	\dot{m}_{ath}
v (EGO sensor)	λ_{meas} (U-EGO sensor)
N	N
p_{man}	p_{man}
\dot{m}_{fi}	
u	

Table 6.1: Measured parameters. The left column shows parameters collected from Trionic T7 over the CAN-bus and the right column shows parameters collected from additional sensors. Also u and \dot{m}_{fi} , which are commanded signals, were collected.

	Weight [g]
Empty canister	1181.28
Time [s]	Adsorbed Fuel
0	153.20
1170	102.50
2340	83.20
3510	72.50
4680	66.05
5850	60.50

Table 6.2: Measurements from the electric scale. The empty weight of the canister and the adsorbed mass of fuel during the experiment.

T7. Matlab also measured the time and produced a trigger signal which should make it possible to merge the sampled analog signals with the digital signals from Trionic T7. Another Matlab shell made the collection of sampled data from the analog signals. The sampling rate of the analog signals from additional sensors was 13 Hz during the experiment.

6.3.2 Experimental Results

The measurements from the electric scale during the experiment is presented in Table 6.2 along with the empty weight of the canister. These measurements are very exact compared with the other measurements.

The experiment showed that it was possible to measure the air mass flow \dot{m}_{ap} and the fuel mass flow \dot{m}_{fp} through the purge control valve and from them calculate the mass concentration μ in order to construct a concentration profile. In Figure 6.6, \dot{m}_{ap} , \dot{m}_{fp} , and μ measured and calculated from the experiment is shown. It can be seen that the concentration profile do not follow the shape of the upper concentration profile in Figure 6.4, which it should be compared with.

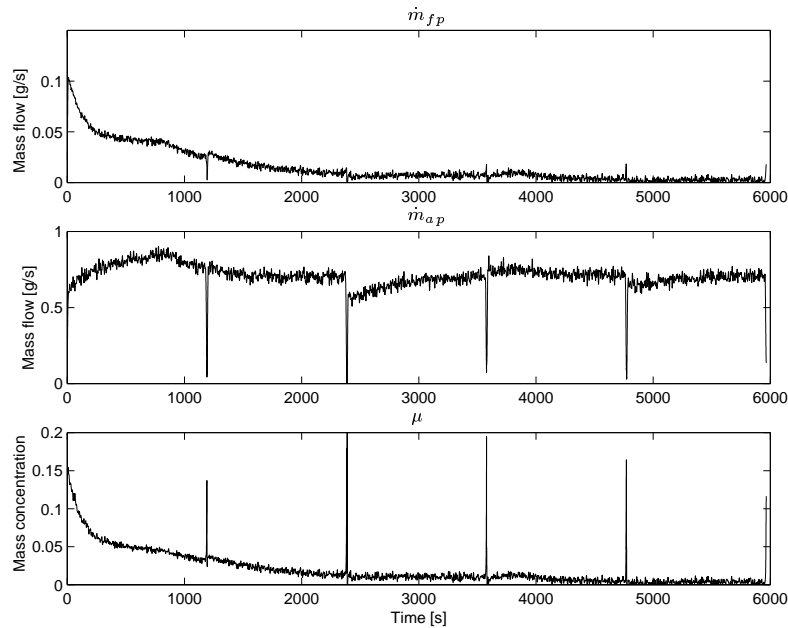


Figure 6.6: Measurement from the experiment. In the upper figure measurement of \dot{m}_{fp} is shown, in the middle figure measurement of \dot{m}_{ap} is shown and in the lower figure the calculated mass concentration μ is shown.

This measured concentration profile looks more like a decreasing exponential function or $\mu(t) \sim Ce^{-at}$. It may be explained by the fact that the canister maybe was just a little more than half full at the start of the experiment. It is known that the canister could give off at least concentration values four times higher than measured here. Another possible explanation is that the test cell was too cold for the canister to be able to give away most of its adsorbed fuel. The weighing of the canister indicates this. As seen in Table 6.2, there is about 40 % of the original fuel amount left in the canister after the experiment.

The spikes in Figure 6.6 come from when the purge control valve is closed. It was not possible to merge the data exactly at these points. The mass flows goes toward zero at these points making it hard to calculate the concentration due to measurement noise.

From \dot{m}_{fp} , the loss of fuel in the canister was integrated. Compared to the measurement on the electronic scale in Figure 6.7, it can be seen that \dot{m}_{fp} is almost correctly measured. This indicates that the method, that is described in Chapter 4, really works.

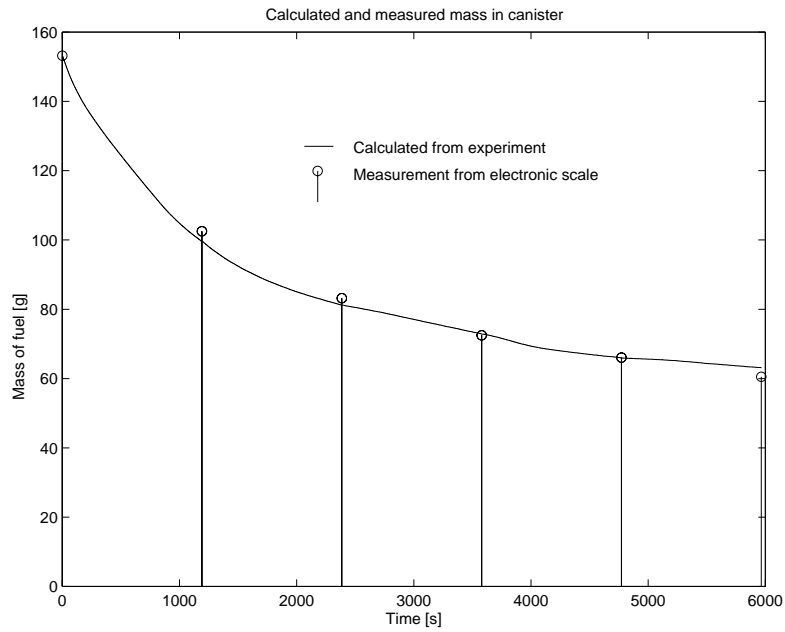


Figure 6.7: Calculated and measured mass of fuel in the canister during the experiment.

Chapter 7

Simulations

Validation of the estimation method in Chapter 4 and the improved fuel control algorithm in Chapter 5 will here be made. The validation is made by simulations of the engine according to the model in Chapter 3 and by using the fuel control algorithm on the engine model. Of course, validation of a method on the model it was based on, do not give the same validity as if it was done on the real system. But on the other hand the model in Chapter 3 has been successfully used by others, without the parts which has been included for the EVAP-system. However that might be, the simulations will at least tell if the method is worth going further with.

The simulations will be made both for an EGO and a U-EGO sensor. In Table 7.1 the values for the proportional and integrating constants K_p and K_i used in the λ -controller is shown. Different values is used depending what kind of λ -sensor we use. Also shown in table 7.1 is the value used for the gain K_μ in the observer of $\hat{\mu}$ from (4.16). The gain K in the observer of p_{man} was never decided since the observer used exactly the same model as it was simulated against and therefore $\hat{p}_{man} = p_{man}$ for every value of K .

	EGO sensor	U-EGO sensor
K_p	0.03	1.2
K_i	0.05	2.9
K_μ	2.5	2.5

Table 7.1: Constants of the fuel control algorithm used in the simulations.

For the simulations, the inputs to the throttle and purge control valve will be controlled according to Figure 7.1 and μ is set to 0.4 if nothing else is told. A value of μ equal to 0.4 is a quite large value, but the carbon canister is fully capable to give away greater concentrations than this. As initiation value of $\hat{\mu}$, 0.3 will be used, simulating that the μ is not fully known. The boost

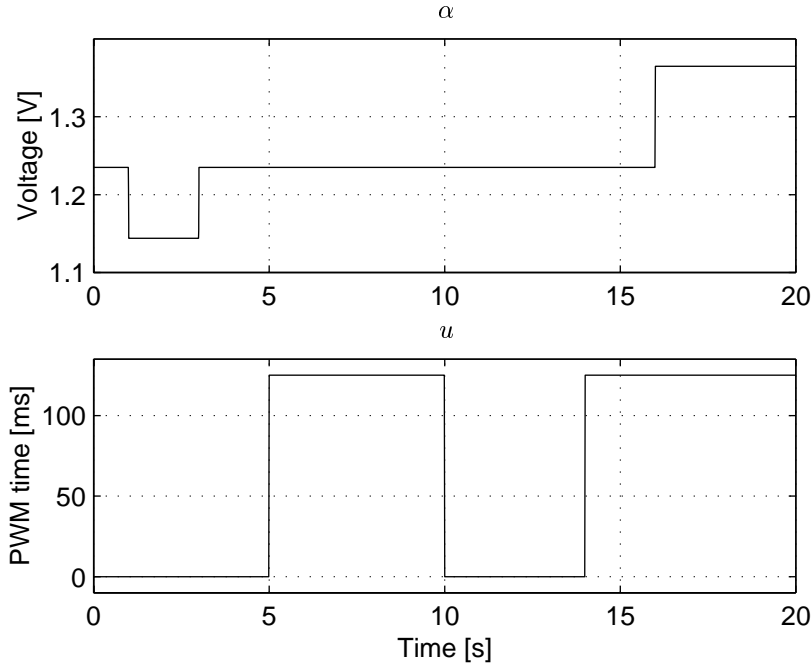


Figure 7.1: Throttle angle α [V] and PWM control signal u [ms] describing the test cycle for the simulations.

pressure from the turbo charger p_{boost} is in the simulations assumed to be close to ambient pressure p_{amb} , and since the turbo charger will not be modeled, p_{boost} is replaced by p_{amb} in Equation (3.7).

7.1 Simple Fuel Control

The engine will first be simulated with no compensation for the extra fuel from the EVAP-system. A simple fuel control algorithm will then be used, only assuming that the gas flow into the cylinders can be calculated from the engine speed N and the intake manifold pressure p_{man} by using the function (3.13) and then use it as an estimate of the air through the intake runners without taking any concern to that some of the gas flow might be fuel. This estimate, denoted \tilde{m}_{ar} , will be used to calculate the required fuel to be injected. The same kind of λ -controller will be used as in the improved fuel control algorithm. The simple fuel control algorithm can be written as

$$\dot{m}_{fi} = \frac{\tilde{m}_{ar}}{(A/F)_s} + d_\lambda$$

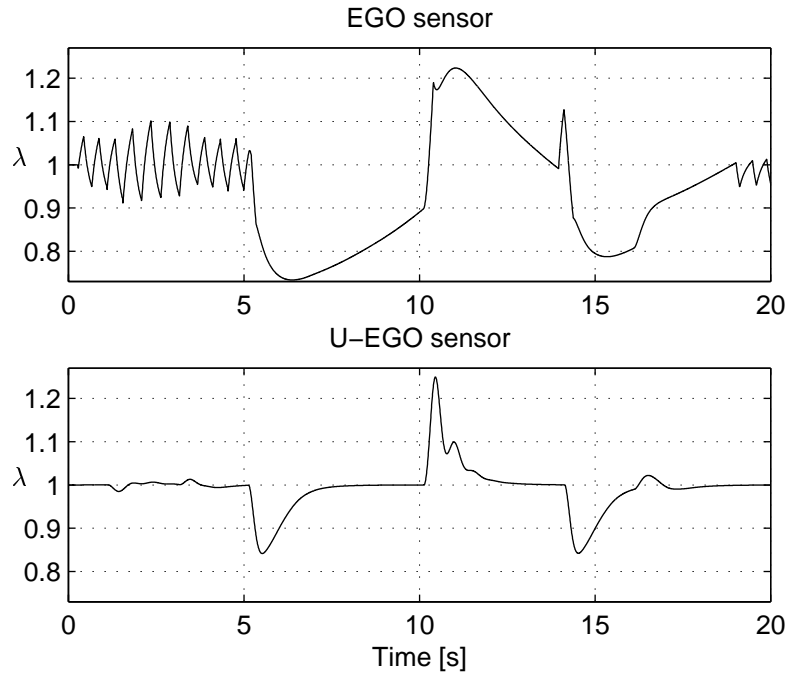


Figure 7.2: Simulation with both an EGO sensor and a U-EGO sensor when a simple fuel control algorithm is used.

In Figure 7.2, λ is shown when using an EGO sensor and a U-EGO sensor respectively and no compensation for the fuel from the EVAP-system is done. It can be seen that the fuel control algorithm handles fast changes in air flow past the throttle well, but it is not able to handle the opening and closing of the purge control valve. For the EGO sensor, λ can not even be stabilized within about 5 seconds. The zig-zag shape of λ in Figure 7.2 comes from the discrete values from the EGO sensor, which makes the λ -controller to perform a so called *limit cycle*, i.e. the oscillation shown.

7.2 Improved Fuel Control

When using the improved fuel control algorithm, shown in Figure 7.3, λ is controlled much better, both for the EGO-sensor and the U-EGO sensor. However, it can be seen that there is still a big deviation of λ from 1 after 5 seconds when the purge control valve is opened for the first time. This is because $\hat{\mu}$ is initially set to 0.3 and it takes some time for $\hat{\mu}$ to reach 0.4 as seen in Figure 7.4. When the purge control valve is closed later, $\hat{\mu}$ in Figure 7.4 is near 0.4 and holds that

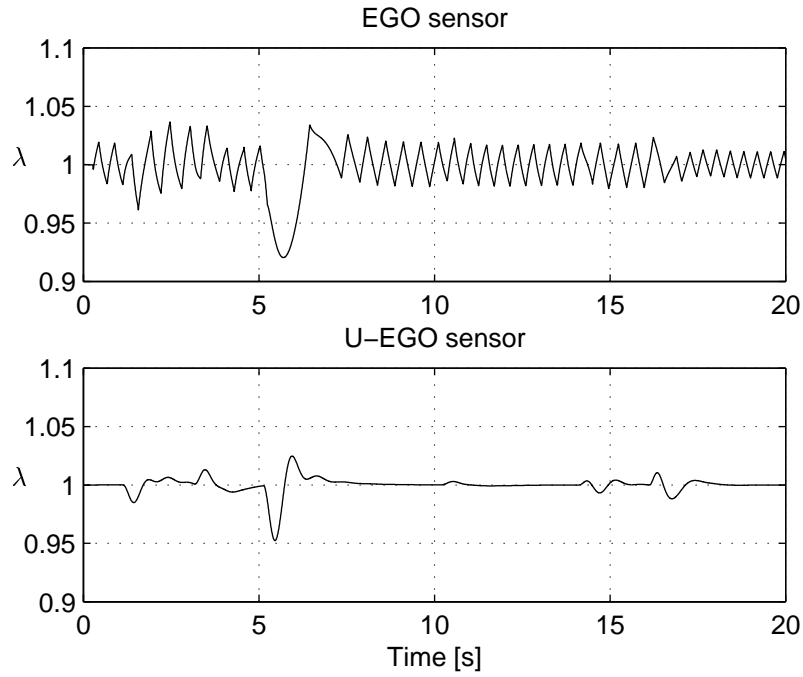


Figure 7.3: Simulation with the improved fuel control algorithm.

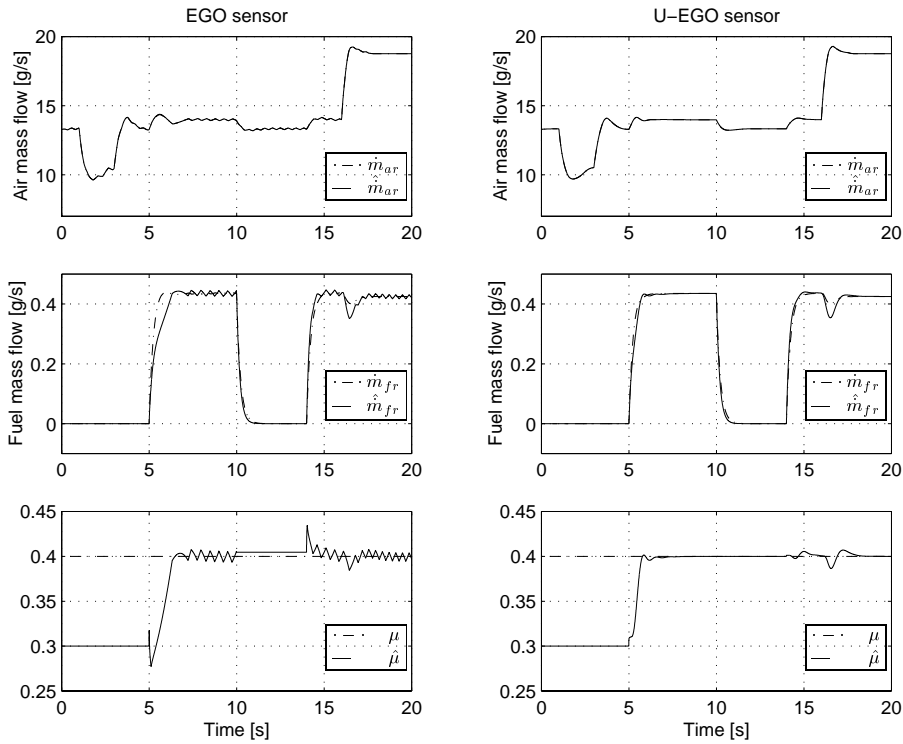


Figure 7.4: Estimations done with the improved fuel control algorithm .

value to the second time the purge control valve is opened. Then no big deviation of λ from 1 is seen in Figure 7.3. The part of the air mass-flow through the intake runners which originates from the EVAP system is small compared to the flow past the throttle and since exactly the same models of the throttle and the intake runners are used in the engine model and the estimation method no difference can be seen between \dot{m}_{ar} and $\hat{\dot{m}}_{ar}$ in Figure 7.4. Differences can be seen both for the EGO sensor and the U-EGO sensor between \dot{m}_{fr} and $\hat{\dot{m}}_{fr}$. This is because $\hat{\mu}$ sometimes deviates from its real value and that the low-pass filter $H(s)$ is used as a simplified model of the manifold. After 16 seconds in the simulation the throttle is opened for the last time. Due to the pressure raise in the intake manifold less vapour is drawn through the purge control valve. This can be seen by the dip in \dot{m}_{fr} at 16 seconds in Figure 7.3. Also the estimate $\hat{\dot{m}}_{fr}$ makes a dip, but this dip is larger due to fact that also the estimation of μ is influenced. The influence in $\hat{\mu}$ comes from the fact that during the pressure raise in the intake manifold there is no steady state.

To avoid that λ deviates from 1 too much the first time the valve is opened, one can open the purge control valve more gently the first time. This is shown in Figure 7.5, where the purge control valve is ramped up under 2 seconds the first time. In Figure 7.6 it can be seen that this strategy improves the control of λ . The estimation of μ does not become any faster by this strategy (and not any slower either) as seen in Figure 7.7 but since the purge control valve is opened more gently, faults in the estimate of μ will not affect the other estimates so much. The λ -controller also have enough time to take care of minor faults.

Until now the simulations has used a constant value of μ . In order to see how well the estimation method is able to follow a varying concentration, μ will be changed to

$$\begin{aligned} \mu &= 0.4 + 0.15\sin(2\pi 0.1t) + 0.01e(t) \\ e(t) &\in N(0, 1) \quad (\text{White noise}) \end{aligned}$$

then, using the strategy in Figure 7.5, the resulting λ becomes as shown in Figure 7.8. From Figure 7.9 it can be seen that $\hat{\mu}$ follows μ when the purge control valve is open, but there is a lag of around 0.2 seconds due to the time delay in λ . This lag makes λ to be less than 1 for a long time, see Figure 7.8. But the varying of μ is quite extreme here. In reality μ will very rarely vary so fast as simulated here. In Figure 7.8 it can also be seen again that the compensation does not work so well when μ is initiated wrong and the purge control valve is opened rapidly.

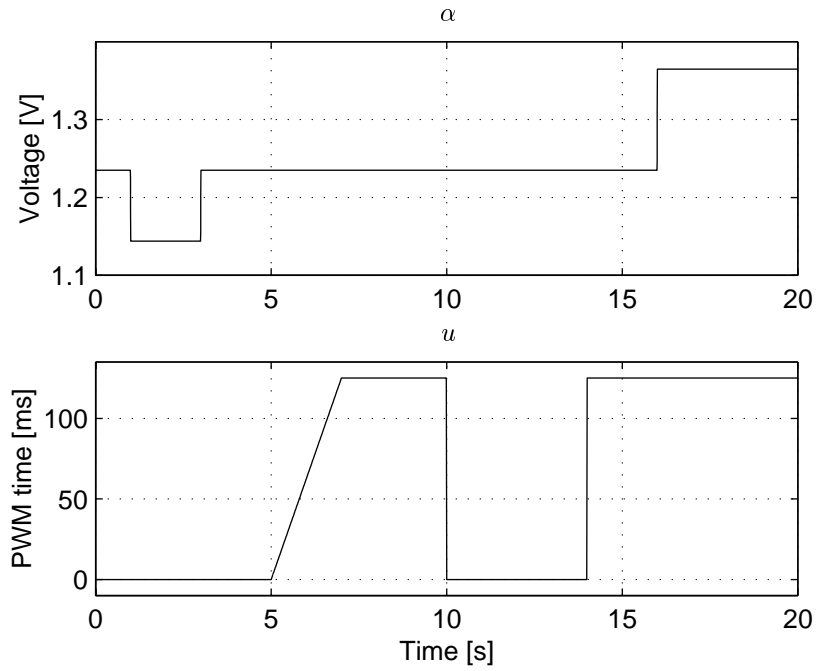


Figure 7.5: Throttle angle α [V] and PWM control signal u [ms] describing the new strategy for the simulations.

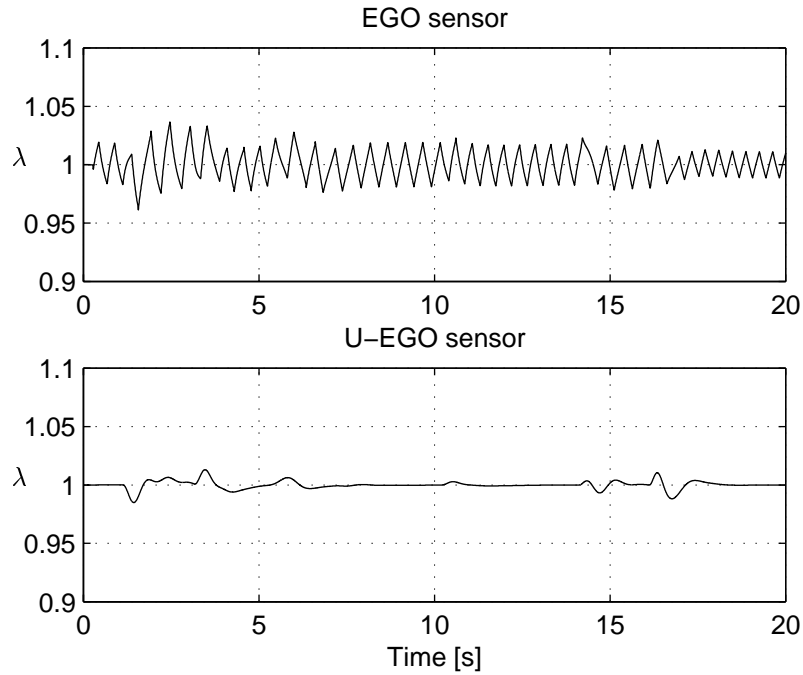


Figure 7.6: Simulation when using a new strategy with the improved fuel control algorithm.

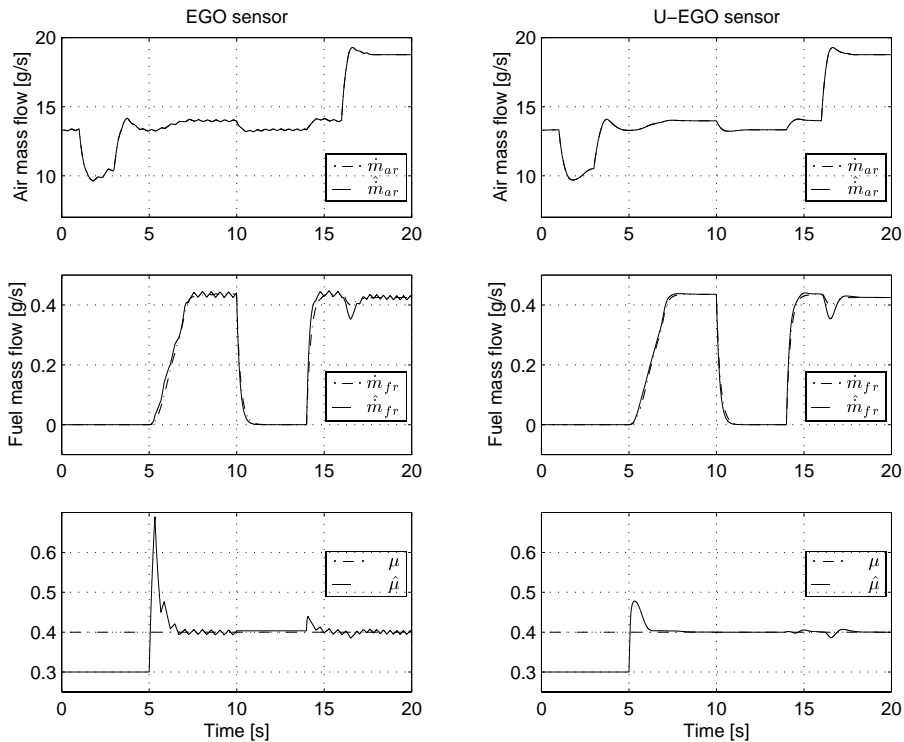


Figure 7.7: Estimations done when using a new strategy with the improved fuel control algorithm.

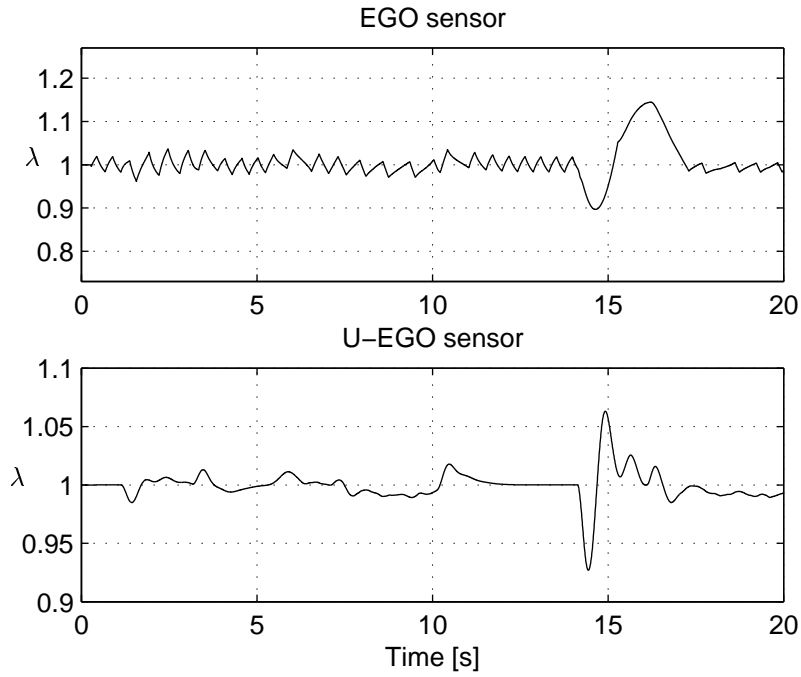


Figure 7.8: Simulation when varying μ and using the improved fuel control algorithm.

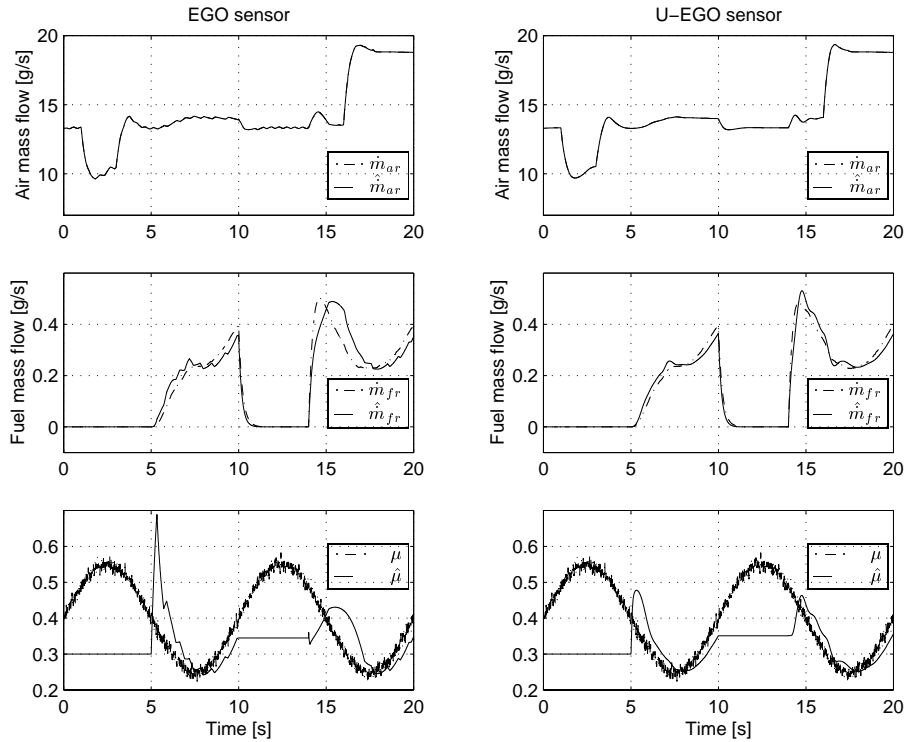


Figure 7.9: Estimations done when varying μ and using the improved fuel control algorithm.

Chapter 8

Conclusions

The exhaust emission control in a car equipped with an evaporative emissions management system can be substantially improved if the fuel vapour flow from the evaporative emissions management system can be estimated.

A method for estimating the fuel vapour flow without making use of any other sensors than standard automotive sensors is developed. The method is based on a physical model of an SI-engine and steady state conditions in the SI-engine. The model of the SI-engine makes use of known physical relations, such as the Ideal Gas Law and Newton's Second Law, but also uses phenomenological relations measured in cases where no good physical relation could be achieved. The estimation method is used in an improved fuel control algorithm. The method has a feature in which the last estimated composition of fuel and air in the vapour, i.e. the concentration, is memorized when the purge control valve controlling the vapour flow from the evaporative emissions management system is shut off.

The improved fuel control algorithm is validated by simulations on the model of the SI-engine. The result shows that the estimations show good agreement with the simulated fuel vapour flow in the engine. The simulation also shows that the exhaust emission control is improved both for a discrete λ -sensor and a continuous λ -sensor. If a strategy is used where the purge control valve is opened gently when the concentration of fuel in the vapour is not known and the purge control valve is opened more rapidly when the concentration is known from previous estimations, the simulation shows very good results. The ability for the estimation method to follow changes in the concentration of the vapours is limited but it is assumed to be adequate for the variations which are present in the evaporative emissions management system.

An approach to model the carbon canister in the evaporative emissions management system was introduced. The carbon canister is the most essential part of the evaporative emissions system as it makes it possible to trap and store evaporated fuel from the fuel tank. However, this approach was not completed but the research gave a better understanding of the physics behind the carbon

canister and the evaporative emissions management system as a whole.

8.1 Further Work and Extensions

Since the validity of the simulations done in this thesis can be questioned, the most essential thing to go further with is to implement the improved fuel control algorithm on a real engine in an engine test cell and validate the method there. Before this can be done, the engine model has to be identified more accurately and some of the parts of the model may have to be improved a little bit. Especially the map over the gas flow through the purge control valve has to be improved.

The physical model over the purge control valve should also be investigated further since the technical specification [7] of the valve supports this model. If a more accurate physical model could be achieved it would give flexibility to adapt the method for different conditions, such as temperature and humidity. Further work to get a good model over the carbon canister is also interesting.

The companies behind the evaporative emissions management system used in this thesis, GM and Delphi-Energy and Engine Management Systems have in a paper [6] proposed a slightly different approach to estimate the vapour flow. They make use of an acoustical sensor, which can measure the concentration in the fuel vapour line from the canister. Their method could be interesting to use in experimental measurements in order to validate the method presented here.

An extension to the method presented here could be to use the estimate of air that goes into the intake manifold through the purge control valve \hat{m}_{ap} as input to the throttle controller in order to make compensation of the extra air that enters the engine when the purge control valve is opened.

A problem that occurred during this work is the difficulty to measure gas flows correctly. Especially when indirect methods are used, where the desired measure has to be calculated from other measured variables. Another problem is that it is difficult to load the carbon canister with fuel quickly so that experiments can be repeated many times.

Bibliography

- [1] C.F. Aquino. Transient A/F control characteristics of the 5 liter central fuel injection engine. *SAE Technical Paper Series*, 1981.
- [2] P W. Atkins. *Physical Chemistry*. Number ISBN: 0-19-855731-0. Oxford University Press, fifth edition, 1994.
- [3] Nicholas P. Cheremisinoff and Paul N. Cheremisinoff. *Carbon Adsorption for Pollution Control*. Number ISBN: 0-013-393331-8. PTR Prentice-Hall, 1993.
- [4] Paul Degobert. *Automobiles and Pollution*. Number ISBN: 1-56091-563-3. Society of Automotive Engineers, Inc, 1995. Translation of “Automobile et pollution”.
- [5] Delphi Energy & Engine Management Systems. *Vapor Canister Outline*, 1996. Technical documentation.
- [6] Myrna C.Sultan et. al. Closed loop canister purge control system. *SAE Technical Paper Series*, (980206), 1998.
- [7] Freudenberg. *Technische Unterlage zur Bemusterung AKF Ventile*, 1994. Technical specifications of purge control valve. In German.
- [8] Elbert Hendricks and Spencer C. Sorensen. Mean value modeling of spark ignition engines. *SAE Technical Paper Series*, 1990.
- [9] J.Glynn Henry and Gary W. Heinke. *Environmental Science and Engineering*. Number ISBN: 0-13-120650-8. Prentice-Hall, second edition, 1996.
- [10] John B. Heywood. *Internal Combustion Engine Fundamentals*. Number ISBN: 0-07-100499-8. McGraw-Hill, McGraw-Hill series in mechanical engineering, international edition, 1988.
- [11] Per-Johan Aronson Ivars Neretnieks and Mats Westermarck. Adsorption - del 2. *Kemisk Tidskrift*, (7):20–25, 1978. In Swedish.

-
- [12] John D. McKenna John C. Mycock and Louis Theodore. *Air Pollution Control Engineering and Technology*. Number ISBN: 1-56670-106. CRC Press, Inc, 1995.
- [13] Matts Karlsson Karl Storck and Dan Loyd. Formelsamling i strömningslära, termodynamik och värmeöverföring. IKP, LiTH, December 1994. LiTH-IKP-S-424. In Swedish.
- [14] C. Åkesson. En grundläggande studie i transientreglering. Master's thesis LiTH-ISY-EX-1913, Department of Electrical Engineering, Linköping University, Linköping, Sweden, February 1998. In Swedish.
- [15] M. Nyberg and A. Perkovic. Model based diagnosis of leaks in the air-intake system of an SI-engine. *SAE Technical Paper Series*, (980514), February 1998.
- [16] Keith Owen and Trevor Coley. *Automotive Fuels Reference Book*. Number ISBN: 1-56091589-7. Society of Automotive Engineers, Inc, second edition, 1995.
- [17] Saab Automobile AB, Saab Automobile AB, Trollhättan, Sweden. *Verkstadshandbok*, swedish edition, 1997. Published by Service Readness, Saab Automobile AB. In Swedish.